

# **DESIGN OF A PHYSICAL HUMAN-ROBOT INTERFACE FOR LIFTING OPERATIONS**

**A Thesis Submitted to  
the Graduate School of Engineering and Sciences of  
İzmir Institute of Technology  
in Partial Fulfillment of the Requirements for the Degree of  
MASTER OF SCIENCE  
in Mechanical Engineering**

**by  
Uğur NALBANT**

**July 2022  
İZMİR**

## **ACKNOWLEDGMENTS**

I would like to express my sincerest gratitude to my supervisor Assoc. Prof. Dr. Mehmet İsmet Can DEDE for his excellent guidance and endless patients during my studies.

I would like to thank my dear friend Kaan Erol KURT for his support and helps.

I would like to thank Güralp Crane and Machinery Corporation for supporting this thesis research.

# ABSTRACT

## DESIGN OF A PHYSICAL HUMAN-ROBOT INTERFACE FOR LIFTING OPERATIONS

In this thesis, the design of a physical human-robot interface for lifting operations which controls the vertical movement of the payload is studied. The new design uses a low stiffness type of admittance control method that is aimed at reducing the surface impact force of the payload and providing better control for the operator while having the option of high stiffness admittance control.

To reduce impact forces by using low stiffness admittance control, a sliding handle mechanism is introduced into the system. This type of design includes springs and bearings to create a low stiffness admittance-type user interface. Mathematical models are developed to calculate spring forces and mechanical strength. According to design requirements and mathematical calculations, the prototype is designed and manufactured. In the tests, it is seen that the spring forces are low, and the sliding motion of the handle is not consistent over different displacements. According to the test results, revisions are done, and the final design of the system is developed. In the final tests, it is seen that the new design of the physical human-robot interface performance is improved and the problem of the sliding motion of the handle is solved. Also, the surface impact forces are reduced with low stiffness admittance control.

Another improvement of the new design is the ability to control the payload with high stiffness admittance control if the user chooses it. With this option, users can control the payload by touching the payload. Having both types of control methods, the user can choose which type of control method to use to handle payload in the factory.

# ÖZET

## KALDIRMA OPERASYONLARI İÇİN FİZİKSEL İNSAN-ROBOT ARAYÜZÜ TASARIMI

Bu tezde, faydalı yükün dikey hareketini kontrol eden kaldırma operasyonları için fiziksel bir insan-robot arayüzü tasarımı incelenmiştir. Yeni tasarımda, yükün yüzey darbe kuvvetini azaltmayı ve operatör için daha iyi kontrol sağlamayı amaçlayan aynı zamanda yüksek dirençlilik admitans tipi kontrol yöntemi seçeneği bulunan, bir düşük dirençlilik admitans tipi kontrol yöntemi kullanılmıştır.

Darbe kuvvetlerini düşük dirençlilik admitans kontrolü kullanarak azaltmak için sisteme kayar kol mekanizması dahil edilmiştir. Bu tasarım türü, düşük dirençlilik admitans tipi bir kullanıcı arayüzü oluşturmak için yaylar ve rulmanlar içermektedir. Yay kuvvetlerini ve mekanik mukavemeti hesaplamak için matematiksel modeller geliştirilmiştir. Tasarım gereksinimlerine ve matematiksel hesaplamalara göre prototip tasarlanmış ve üretilmiştir. Testlerde, yay kuvvetlerinin düşük olduğu ve kolun kayma hareketinin farklı yer değiştirmelerde tutarlı olmadığı görülmüştür. Test sonuçlarına göre revizyonlar yapılmıştır ve sistemin nihai tasarımı geliştirilmiştir. Son testlerde, fiziksel insan-robot arayüz performansının yeni tasarımının iyileştirildiği ve kolun kayma hareketi probleminin çözüldüğü görülmektedir. Ayrıca düşük dirençlilik admitans kontrolü ile yüzey darbe kuvvetleri azaltılmıştır.

Yeni tasarımın bir başka iyileştirmesi, kullanıcı isterse, yüksek dirençlilik admitans kontrolü ile yükü kontrol etme yeteneğidir. Bu seçenek ile, kullanıcı yüke dokunarak yükü kontrol etme imkanına sahiptir. Her iki tür kontrol yöntemine sahip olan kullanıcı, fabrikada yükü taşımak için hangi tür kontrol yöntemini kullanacağını seçebilir.

*I dedicate this thesis to my dear parents, Nilgün and Hasan NALBANT*

# TABLE OF CONTENTS

LIST OF FIGURES .....	viii
LIST OF TABLES .....	x
CHAPTER 1. INTRODUCTION .....	1
1.1 . Thesis Objective and Motivation .....	3
1.2 . Main Contributions .....	4
1.3 . Thesis Outline .....	4
CHAPTER 2. LITERATURE REVIEW .....	6
2.1. Overview of Control Methods on Physical Human-Robot Interfaces ....	6
2.2. Overview of Physical Human-Robot Interface for Lifting Operations ..	8
2.3. Developments About Electrical Manipulators.....	10
2.4. Conclusion .....	14
CHAPTER 3. DESIGN OF THE PHYSICAL HUMAN-ROBOT INTERFACE .....	16
3.1. Working Principle of the Lifting System with Physical Human-Robot Interface .....	17
3.2. Design Requirements .....	21
3.3. Mathematical Model .....	23
3.4. Design of the Load Carrying Element .....	27
3.5. Design of the Sliding Handle.....	28
3.5.1. Sensor Selection .....	29
3.5.2. Prototype Design.....	29
CHAPTER 4. FINAL DESIGN AND TESTING OF THE PHYSICAL HUMAN- ROBOT INTERFACE .....	33
4.1. Testing of the Prototype Design .....	33
4.1.1. Force Test of the Prototype .....	34
4.1.2. Displacement Test of the Prototype .....	35

4.1.3. Mass Measurement Test of the Prototype.....	36
4.1.4. Mass Measurement Test of the Wire Rope System .....	37
4.1.5. Discussion About Prototype Test Results.....	40
4.2. Final Design of the User Interface .....	41
4.2.1. Improvements.....	41
4.2.2. Final Design .....	41
4.3. Test and Results of the Final Design .....	46
4.4. Surface Impact Test with Using Both Control Methods.....	48
4.4.1. High Stiffness Admittance Control Test.....	50
4.4.2. Low Stiffness Admittance Control Test.....	51
4.5. Discussion About Final Design Test Results.....	51
CHAPTER 5. CONCLUSION .....	53
5.1. Future Works .....	54
REFERENCES .....	55

# LIST OF FIGURES

<b><u>Figure</u></b>	<b><u>Page</u></b>
Figure 1: Example of a crane system that uses wire rope.....	1
(Source: GURALP Crane and Machinery, 2017) .....	1
Figure 2: Example of a crane remote controller. ....	2
(Source: GURALP Crane and Machinery, 2017) .....	2
Figure 5: Example of a pneumatic manipulator with mass dial. ....	9
(Source: Dalmec Industrial Manipulators, 2022).....	9
Figure 6: Human power amplifier for lifting load (Source: Kazerooni, 1999).....	11
Figure 7: Lift actuator controller handle (Source: Stockmaster, 2008) .....	12
Figure 8: Apparatus for lifting and moving object (Source: Zanardi, 2005).....	13
Figure 9: Pulley assembly in the motor system. (Source: Zanardi, 2005).....	14
Figure 10: Working principle admittance type of user interfaces .....	17
Figure 11: Control scheme of the lifting system.....	18
Figure 12: Design of the construction.....	20
Figure 13: Manufactured picture of the construction. ....	21
Figure 14: Example of electrical physical human-robot interface.....	22
(Source: Indeva Intelligent Devices for Handling, 2022) .....	22
Figure 15: Load carrying element of the human-robot interface.....	24
Figure 16: Sliding handle schematic.....	26
Figure 17: Section view of prototype design .....	30
Figure 18: Picture of the assembled prototype sliding handle mechanism.....	32
Figure 19: Test system of the prototype human-robot interface.....	34
Figure 20: Example of a Crane System .....	37
Figure 21: Wire Rope System.....	38
Figure 22: Seesaw Mechanism for Mass Measurement in Cranes .....	39



<b><u>Figure</u></b>	<b><u>Page</u></b>
Figure 23: Front (left) and isometric (right) view of the human-robot interface.....	43
Figure 24: Section view of the final design. ....	44
Figure 25: Final product picture of the physical human-robot interface .....	45
Figure 26: Assembled picture of the lifting system with human-robot interface .....	46
Figure 27: Surface Impact Test System.....	49
Figure 28: High Stiffness Admittance Control Method Surface Impact Test .....	50
Figure 29: Low Stiffness Admittance Control Method Surface Impact Test.....	51

# LIST OF TABLES

<b><u>Table</u></b>	<b><u>Page</u></b>
Table 1: Numerical design requirements.....	23
Table 2: Non-numerical design requirements.....	23
Table 3: Design properties of the load carrying bar. ....	28
Table 4: Description of the sliding handle mechanism prototype elements.....	31
Table 5: Force test results of the prototype design .....	35
Table 6: Displacement test results of the prototype design .....	35
Table 7: Mass test of the prototype design. ....	36
Table 8: Mass test of the crane system. ....	39
Table 9: Force test results of the final design of the physical human-robot interface.....	47
Table 10: Displacement test results of the final design of the physical human-robot interface.....	47
Table 11: Mass measurement test of the final design.....	48

# CHAPTER 1

## INTRODUCTION

In the industry, most of the loads are handled by human operators. Handling is done in three steps: Lift, Adjust and Place. Humans cannot carry out lifting operations of more than 23 Kg according to European Agency for Safety and Health (OSHA 2009). Since humans are restricted in the first step of handling, industry solves this problem by using machines.

For lifting operations, the use of a wire rope system is quite common since it can be wrapped on a drum or a pulley to adjust lifting height and is safe enough to use near humans. In industry applications, wire ropes are commonly used in cranes as a connection between the hook system and the power system to deliver lifting forces one from another. In Figure 1, the usage of the wire rope system in cranes is given.



Figure 1: Example of a crane system that uses wire rope.  
(Source: GURALP Crane and Machinery, 2017)

This power system is controlled by humans via a controller which is placed near the system and usually includes a button or in some cases joysticks, to give a command to the power system to lift the payload up and down direction. These controllers usually

have got two stage inputs which are first and second speed inputs, which adjust the speed of the lifting operations. Figure 2 is an example of a crane remote controller system that is used in the industry. These user interface controllers control the vertical speed of the load but can provide only two different speed option.



Figure 2: Example of a crane remote controller.  
(Source: GURALP Crane and Machinery, 2017)

To increase control, the user needs to be near the lifted load and adjust its rotation by using ropes or his own hands. Since one hand of the user controls the load, it becomes difficult to control the controller with the other hand. To solve this problem, the use of a remote controller is needed, or designers can place the controller on the hook assembly so that the user can use it with one hand while the other hand can control the load.

To increase speed, first of all, users should gain access to more than two-speed options to control the load safely. For this reason, the analogue control input is needed to control the speed at various levels. In the market, this solution includes a potentiometer which is connected to joysticks or a loadcell that is connected to a handle to control the input.

With this type of need, a variety of physical human-robot interfaces started to be used in the industry. These systems have got two things in common: They all can be used with 1 hand, and they have got a wide range of control in terms of lifting speed.

The problem with these systems is controlling the payload when it is touched to the ground. These systems control the vertical movements of the payload by measuring the vertical forces on the physical human-robot interface by using a force sensor. The operator lifts the load by creating a vertical force on the interface. When there is an external force that is acting on the human-robot interface such as a reaction force from the ground, this system can create unwanted movements and controlling such a system becomes harder.

Another problem with electrical lifting machines is reading the payload mass. In electrical lifting machines, the payload mass is measured by measuring the wire rope force on the system. This method may cause the wrong measurement because wire rope tension could increase as the wire rope's vertical angle changes.

## **1.1. Thesis Objective and Motivation**

Lifting mass limit is often overlooked by the operators and managers, but the risk of injury is still present. Even though there are lifting machines for the operators to use, if operators cannot control the load efficiently or in a desired way, operators tend to use his/her body to handle the load. Designing a system that can be used to assist operators to handle the load with minimal effort is the main objective of this thesis. To achieve this goal, the below achievements need to be done:

1. Making a control interface that is close to the lifted load and can be controlled with one hand with less effort.
2. User interface should support high and low stiffness admittance control methods for different handling processes.
3. System should not need adjustment for lifting different loads and conditions unless it is desired by the user.

## **1.2. Main Contributions**

The main contributions of this thesis are as follows:

1. Implementation of a solution that reduces the surface impact and oscillations when the payload is placed on a surface.

To deal with surface reaction force when the payload contacted to the ground, the use of a sliding handle design is proposed. The sliding handle design aims to dampen the reaction force when the payload touches to the surface.

2. Design of a new human-robot interface that can measure the payload mass at a location close to the payload.

A common way to measure payload mass is to place a load sensor that measures the wire rope tension in the system. There are different types of patents and designs for this type of measurement but the tension in the rope is not the same as the payload mass. To eliminate this problem, a load cell is directly mounted to the hook on the new design so that the mass of the payload is directly transmitted to the load cell.

## **1.3. Thesis Outline**

There are 5 chapters in this thesis: Introduction, Literature Review, Design of the Physical Human-Robot Interface, Final Design and Testing of the Physical Human-Robot Interface, and Conclusion.

In Chapter 2, information about physical human-robot interfaces that are used in the industry and literature review about admittance control systems are given. These systems are used with the operator and aim to increase payload handling speeds in the factory. After the information, development in these systems and problems with current technology is addressed.

In Chapter 3, the design of the physical human-robot interface and design processes are covered. These design processes include the working principle of the

system, the design criteria, mathematical models, and sensor and material selection. After these selections, the design of the prototype is presented.

In Chapter 4, testing of the prototype of the sliding handle mechanism that is used in the physical human-robot interface and the final design of the system is given. This chapter includes testing of the prototype, test results and improvements in the system, after that, the final designs of the user interface and the final design of the lifting system are covered. With the final design, surface reaction force tests are conducted.

In Chapter 5, the conclusion of this thesis is given.

## **CHAPTER 2**

### **LITERATURE REVIEW**

In this section, the results of the research and industrial solution on the human-robot interfaces for lifting operations are given. In the first section, an overview of control methods that are used in the physical human-robot interfaces is given. Then an overview of physical human-robot interfaces and the invention of a new type of lifting the machine called manipulators is given. After that invention of electrical manipulators and their various designs are examined. Finally, the section is completed by giving the result of a literature review on the physical human-robot interface for lifting operations which will be a guideline for a new interface to be designed.

#### **2.1. Overview of Control Methods on Physical Human-Robot Interfaces**

To control a robot with a physical human-robot interface, there are two types of controller methods. In impedance control, a human initiates a motion of the system and a restriction force can be generated by the system to be applied to the human (Hogan 1989). In the admittance control, the user applies force to the system which is measured by the system's sensors and accordingly a motion is generated by the system (Adams and Hannaford 1999). Depending on the environment stiffness, both control options can be chosen to create the best performance, this phenomenon is illustrated in Figure 3.



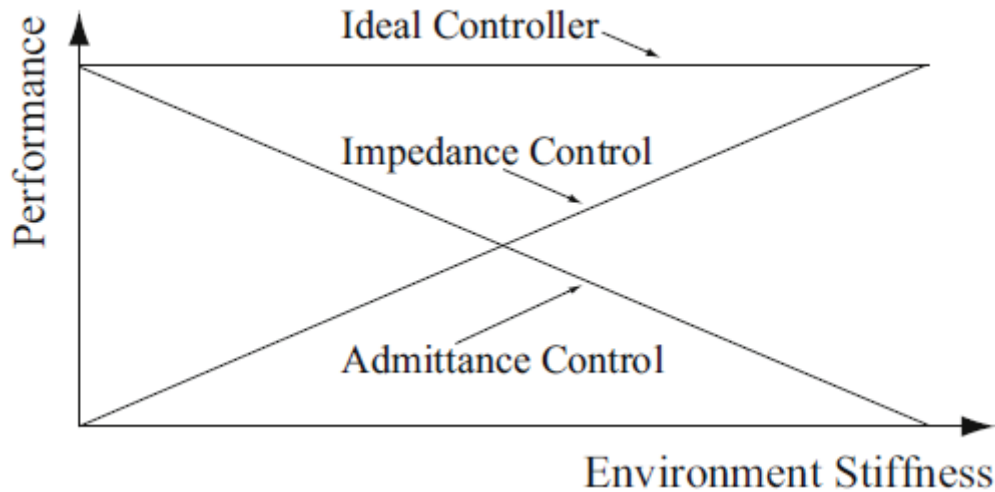


Figure 3: Performance Review of Admittance and Impedance Control for Different Environment Stiffness (Source: Ott, Mukherjee and Nakamura, 2015)

A Hybrid control system is proposed to create an ideal controller for a changing environment stiffness in A Hybrid System Framework for Unified Impedance and Admittance Control (Ott, Mukherjee, and Nakamura 2015). In this paper, the system is a 6 degree of freedom system but to evaluate the performance of both control systems, the test is conducted at 1 degree of freedom motion. Impedance control resulted in low oscillation when there is a stiff contact but high steady state error in free space, on the other hand, admittance control resulted in high oscillations in stiff contact but has a good position accuracy in free space. To adapt to changing stiffness in the environment a control method is proposed and tested. The solution is to change the duty cycle of the system with the stiffness of the environment and resulted in high performance in both low and high environment stiffness. But the main problem with this approach is that the environment stiffness should be well studied to use this method.

Admittance control is widely chosen in industrial products since admittance control system aims to lower the inertia of the heavy machines to enable them to control by human forces. To control a system with admittance control, a force sensor is placed serially between the human operator and the system. This approach divides the dynamics of the system into pre-sensor and post-sensor robot dynamics as is illustrated in Figure 4.

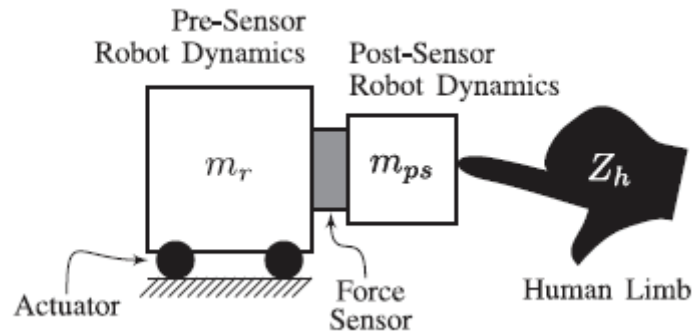


Figure 4: General Illustration of Admittance Control Method for Physical-Human Robot Interface(Source: Keemink, van der Kooij, and Stienen, 2018)

This post-sensor part reacts with the environment or the human limb dynamically and post sensor dynamic reaction will result in the force readings in the force sensor. The human part of the system impedance can be treated as unknown, but the rest of the system dynamics can be calculated. Although this method can be implemented in haptic devices that are used in teleoperation applications, If the system is a handling machine, this post sensor part dynamic will change and should be treated as unknown. As stated in Admittance control for physical human–robot interaction (Keemink, van der Kooij, and Stienen 2018), If this change is purely inertial, a force control method can compensate for this inertial change and have a good admittance control system. On the other hand, this post-sensor robot dynamic change includes an impedance change of the system and admittance control of the system can be unstable.

## 2.2. Overview of Physical Human-Robot Interface for Lifting Operations

In the industry, systems started to appear with admittance type of control which is called manipulators hence the name come from the method that which the user manipulates the system by using his/her hand. This system is introduced to the industry with the invention of a balanced assembly (Olsen 1964), which enables balancing the mass of the load by using actuators. For 30 years, these actuators were pneumatic pistons that generate balancing force in the system. This method can lift a specific load with a

pre-determined mass and shape. Over the years engineers began to use mass balancer dial in the system to adjust piston force on the system so that it can lift different loads. In Figure 5, an industrial example of a pneumatic manipulator is given.

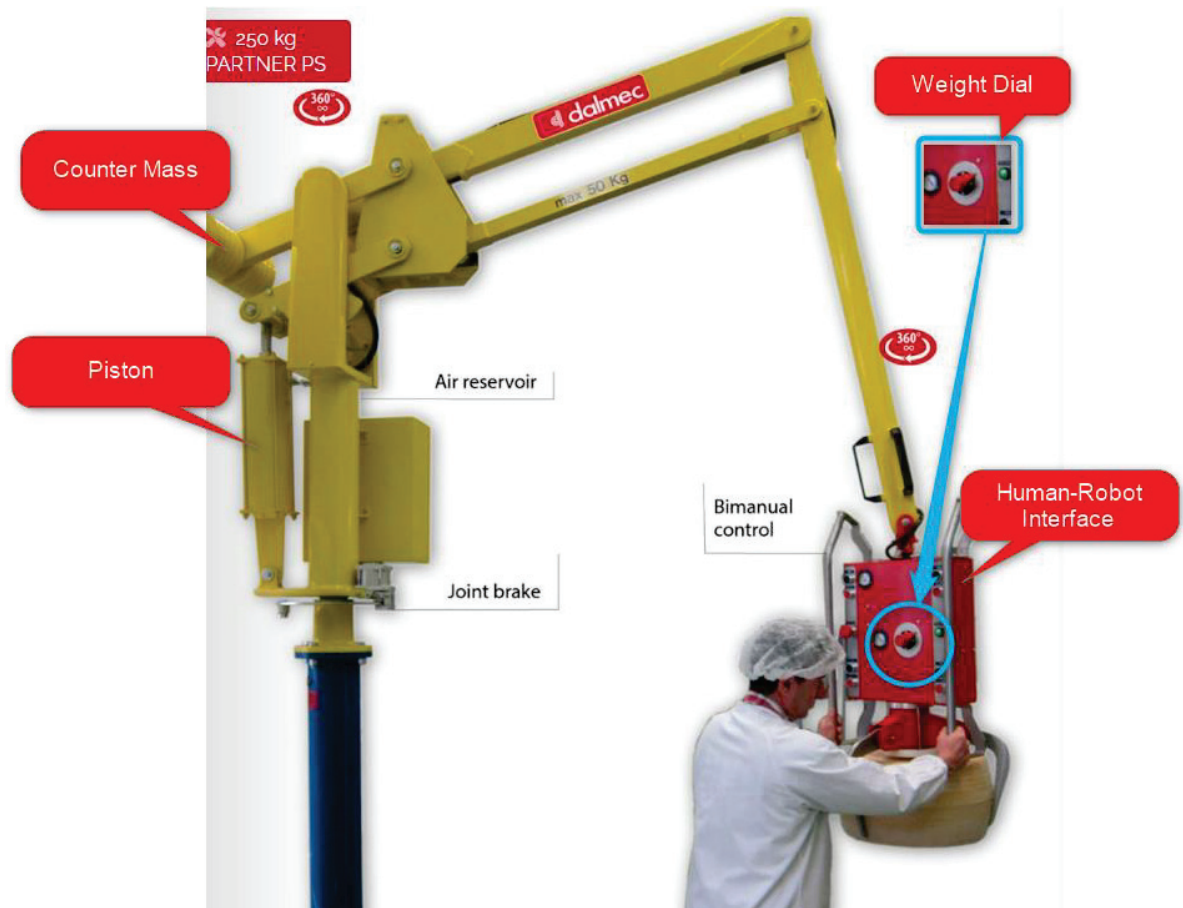


Figure 5: Example of a pneumatic manipulator with mass dial.  
(Source: Dalmech Industrial Manipulators, 2022)

In Figure 5, the counter mass and the piston force are creating a balancing force on the payload that counters the gravitational forces over the payload and the construction. Payload movement is initiated by the operator by exerting force on the human-robot interface. The mass dial on the system tunes the piston force for different payload masses. But different payload scenario problem is solved properly by using electrical manipulators.

### 2.3. Developments About Electrical Manipulators

With the development in electrical motor technologies, a new type of manipulator was invented by using an electric motor and uses sensors to determine the lifted load and human force on the system (Kazerooni 1999). This technique uses wire rope as a connection between the power system and the hook assembly instead of mass balancing with the pistons. This non-rigid connection between the payload and the power system enables the user to have got more flexibility with the control of the load. Since there are no heavy links, the system can move faster and quicker. Wire rope system has got big disadvantage over the fixed link is that it can be slacked and lose control, but this problem is easily solved with the sensors. With the help of electrical sensors and controllers, the slack problem was solved with a slack sensor designed by Kazerooni. (Kazerooni 2003). Also, since the system is electrically controlled and a sensor can be placed so that the vertical position of the hook can be known and by that position virtual limits can be implemented to the system. With this virtual limits, vertical load speed can be automatically slowed down.(Stockmaster 2008).

This designed system uses human forces to move in the lateral direction as it slides on the rails and servo motor power to move vertical direction. As you can see in Figure 6 human controls are connected to the hook assembly so that the user can be near the lifted payload to control and Figure 7 shows an example of a controller handle that is used in the electrical manipulators.

In Figure 6, number 13 is the wire rope that transmits the lifting force from the motor to the lifting interface which is numbered 16. Number 26 is the user interface where the user uses force to give lifting speed and direction to the controller. To calculate the mass of the lifted payload, the system measures motor current in this design.

Another user interface method that is used in the electrical manipulators is shown in Figure 7. This design includes a fixed handle that measures the human force on the grip and, up-down buttons so that the user can control the vertical movement more accurate.

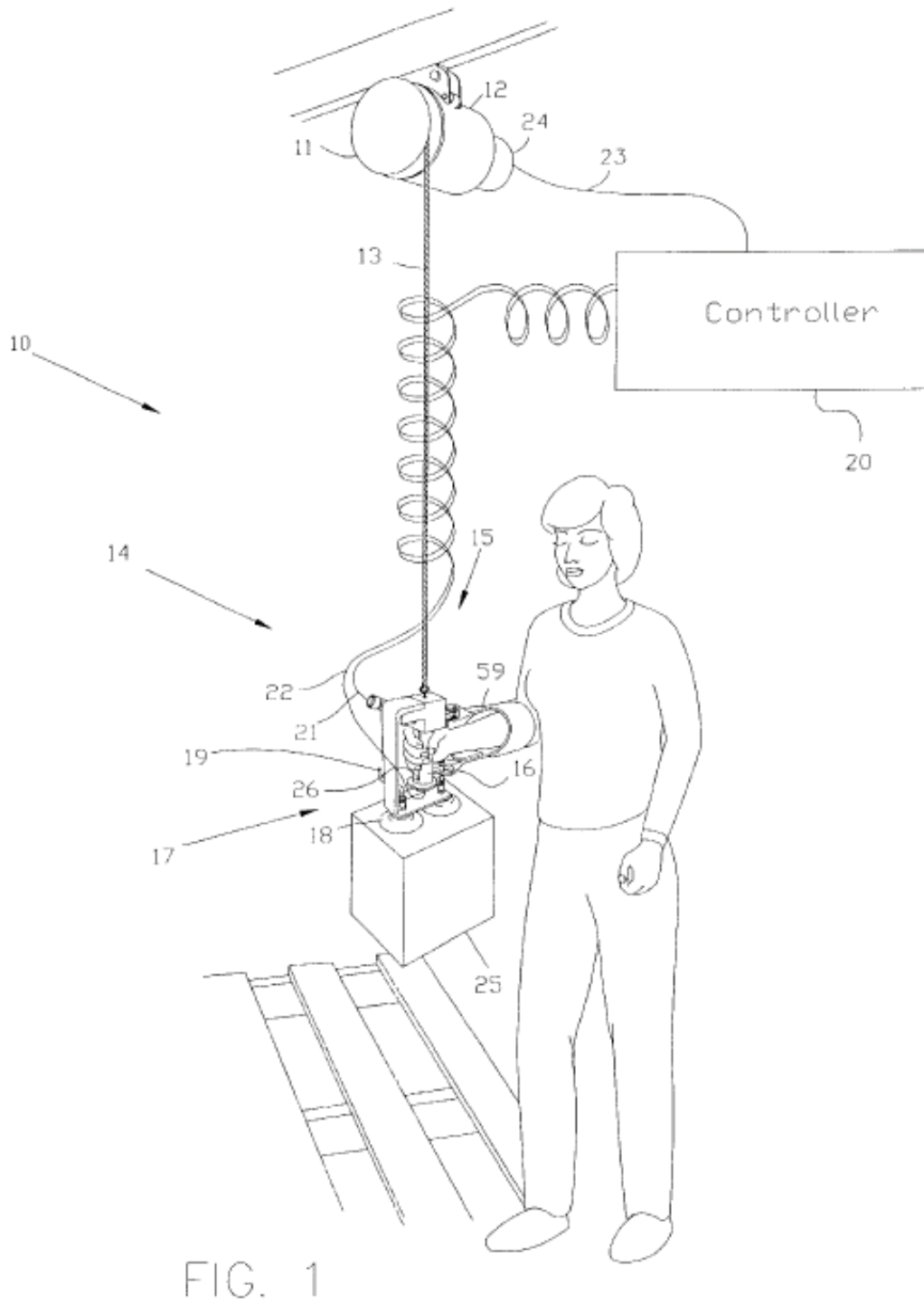


Figure 6: Human power amplifier for lifting load (Source: Kazerooni, 1999)

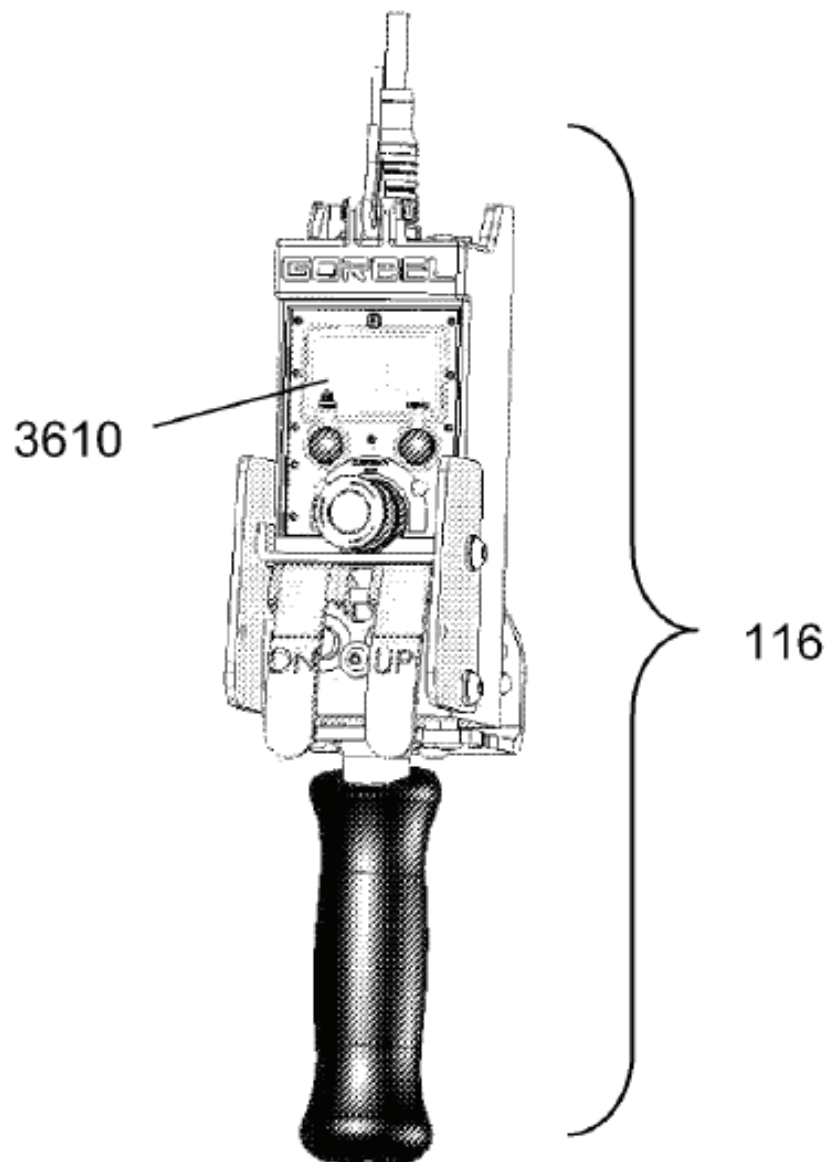


Figure 7: Lift actuator controller handle (Source: Stockmaster, 2008)

Another method for the electrical manipulator is like an overhead crane system that has a motor for the motion along each of the three axes (Zanardi 2005). With this system, all the movement is done with the help of motors so that humans exert the least effort in the handling processes. The problem with this approach is making a human interface so that it can control all three axes of motion. To solve that method, wire rope angles are measured as seen in Figure 8 and Figure 9. Engineers place four pulleys (number 25) in the motor assembly that measures the wire rope angle as it leaves the motor system. When the user tries to move the object, wire rope pushes these pulleys and

creates a reaction force on that pulley. Then according to this force reading motors in response to lateral movements are engaged.

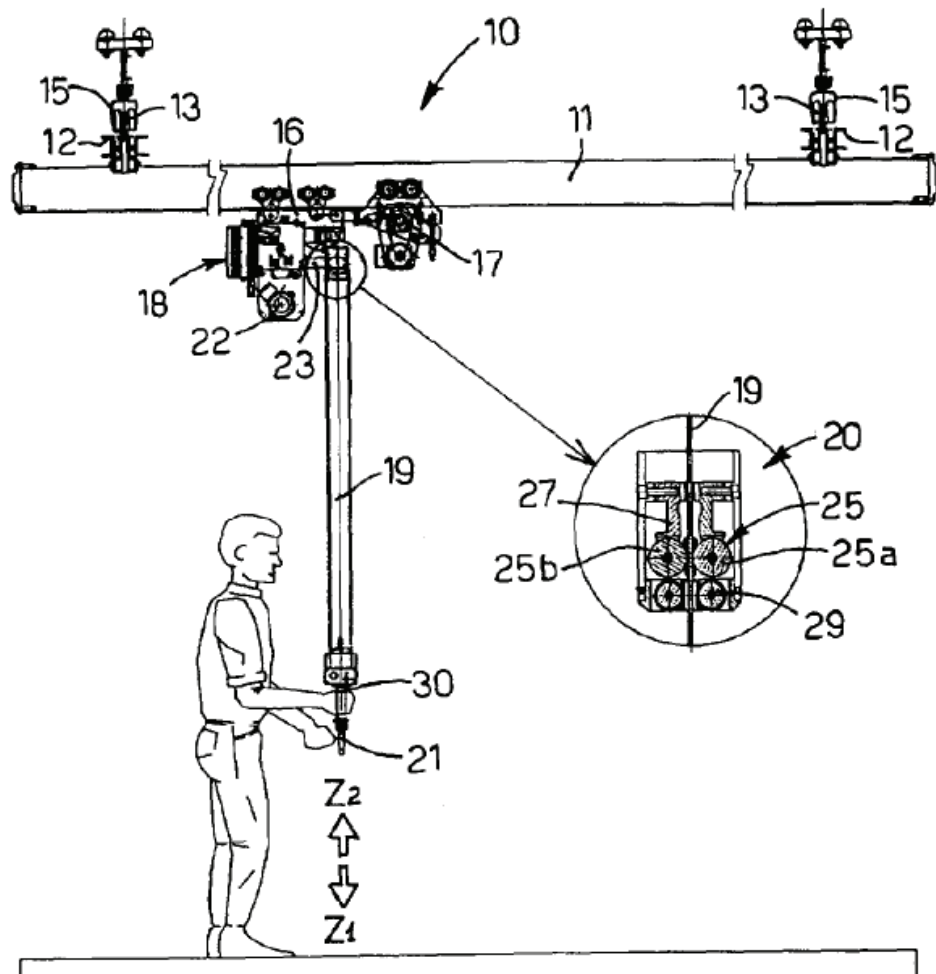


Figure 8: Apparatus for lifting and moving object (Source: Zanardi, 2005)

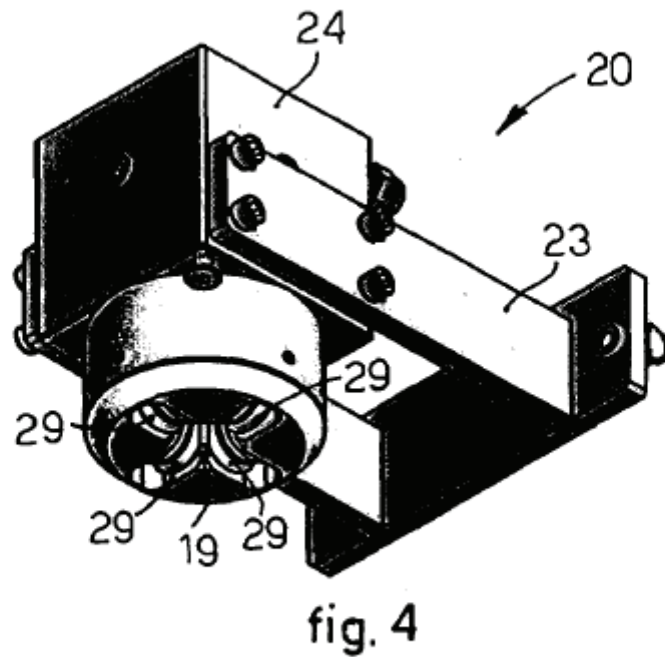


Figure 9: Pulley assembly in the motor system. (Source: Zanardi, 2005)

## 2.4. Conclusion

All these systems use admittance control on their motion to lift the payload up and down. This method is suitable for moving the load but when it is contacted to the surface, it can be hard to control the payload since surface stiffness is unknown and most of the cases it is a high stiff contact. To avoid that problem, a solution is to add buttons to the system that slow down the speed so that because of the minimized impact forces, the surface reaction force will not be in the undesired magnitudes. Another method is to turn off the admittance control and have an up and down button on the system so that it can be moved at a constant speed to avoid an impact force. All these solutions add complexity to the system since it requires the user to react according to the payload position relative to the surface.



To sum up, there is still room for improvement in this system so that users can be more comfortable when using this product.

## CHAPTER 3

### DESIGN OF THE PHYSICAL HUMAN-ROBOT INTERFACE

In the previous section, two major products are examined, which can be classified as pneumatic and electrical. Although pneumatic systems are advantageous in terms of price, they do not meet the design criteria as they are designed to lift a constant mass. To eliminate this problem electrical systems are selected. Electrical motors can control their torque and speed output without needing any input from the user. By considering this feature, electrical motors are selected and hence, the physical human-robot interface is electrically controlled in this study.

Electrical manipulators in the industry introduced force readings to use admittance control. Admittance control type human interfaces have a fixed handle and measure the human forces on that handle for control purposes. Depending on the forces that are exerted on the handle, vertical movement speeds are controlled but the force sensor has high stiffness. This type of approach is easy to use for the operators but there is a problem when the payload contacts the surface. Since the system works with the vertical forces that are exerted on the handle, when the payload touches the surface, the surface reaction forces because of the impact may result in unwanted forces to be measured on the handle and may cause unwanted vertical movement inputs into the system and the admittance control systems performance is worsen when the environment is a high stiffness environment. (Ott, Mukherjee, and Nakamura 2015)

To overcome this problem, a low stiffness force reading admittance control type of design is introduced as a human-robot interface. To use this type of control, the sliding handle method is used with linear bearings and springs. In this way, the operator slides the handle in the desired direction and depending on the displacement of the handle, the system's vertical speeds changes. On the other hand, the high stiffness force reading admittance type of control is more neutral and comfortable to get used to controlling. In Figure 10, the working principles of both systems are given.

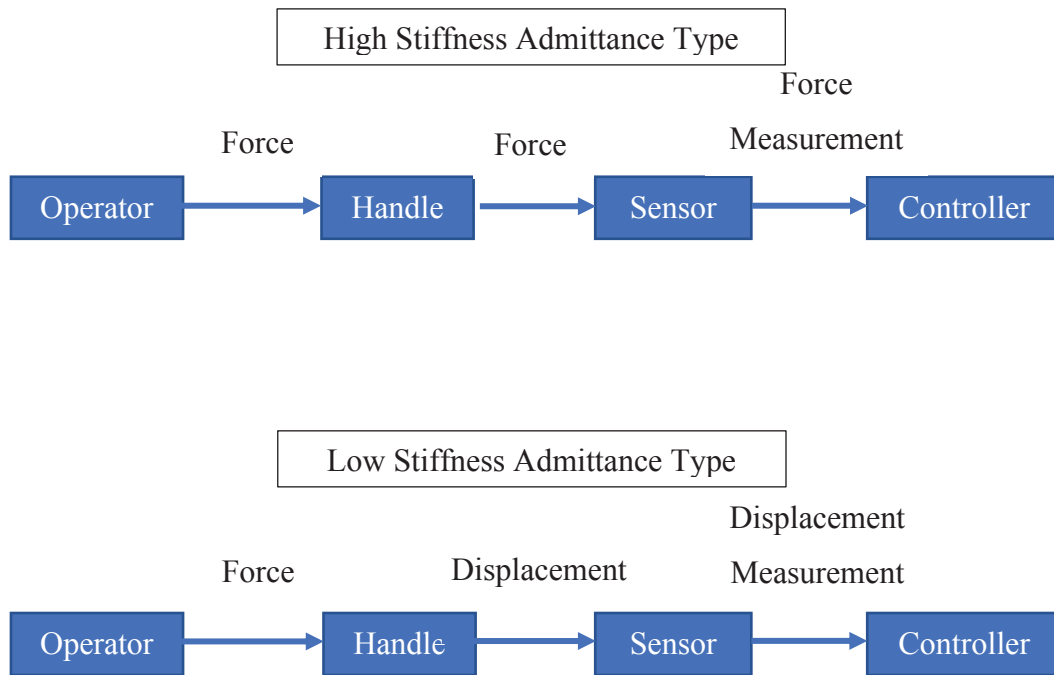


Figure 10: Working principle admittance type of user interfaces

To use both control systems' advantages, a loadcell which is connected to the hook is used. With the help of the loadcell, the system can measure the forces which are acting on the payload and determine desired vertical movement by measuring the human forces acting on the payload.

### 3.1. Working Principle of the Lifting System with Physical Human-Robot Interface

The lifting system consists of three main parts: power system, construction, and the physical human-robot interface. The power system includes a motor and reduction gear assembly responsible for providing lifting force, a drum which is connected to the output shaft of the reduction gear that wire rope winds, a motor controller to control the motor actions, and a programmable logic controller (PLC) to control the lifting operation according to physical human-robot interface signals. The control schema of the system is given in Figure 11.

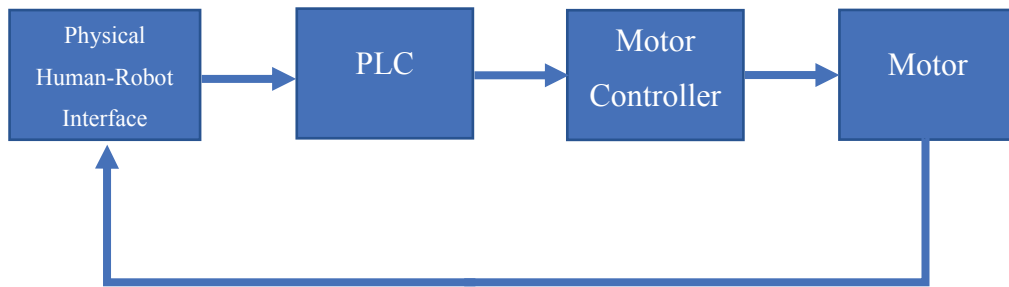


Figure 11: Control scheme of the lifting system

The physical human-robot interface provides the lifting speed and direction signals to the PLC. Depending on the control method these signals change. For low stiffness admittance control, displacement of the handle from its neutral position corresponds to vertical speed and direction demand from the operator. For high stiffness admittance control, it is activated by pressing a button. When the button is pressed, a loadcell reads the mass of the payload and stores that value in the PLC. After that operator force on the payload changes the force reading on the loadcell and depending on that change vertical speed and direction are calculated in PLC. According to these sensor signals PLC will send commands to the motor controller to desired speed values from the motor. The motor controller uses its own control algorithms to control the motor rotational speed according to desired speed input from the PLC. This way power system can lift different payloads without needing any adjustments.

The construction of the system consists of two revolute joints that are perpendicular to the ground. These joints are responsible for the horizontal movement of the payload, and they are not connected to any actuator. The design of this system can be seen in Figure 12.

In Figure 12: Components and their features are given below:

1. First arm: The main arm of the system that is rotating in the horizontal direction with respect to the mast. The power system and second arm are connected to this arm.
2. Second arm: Second arm of the system that is connected to the first arm and rotates in the horizontal direction with respect to the first arm.

3. Power system: Responsible for generating lifting force according to physical human-robot interface signals. Motors, reduction gear, drum, PLC and motor controller are contained in this assembly.
4. The mast: Connects the first arm to the ground.
5. First revolute joint
6. Second revolute joint.

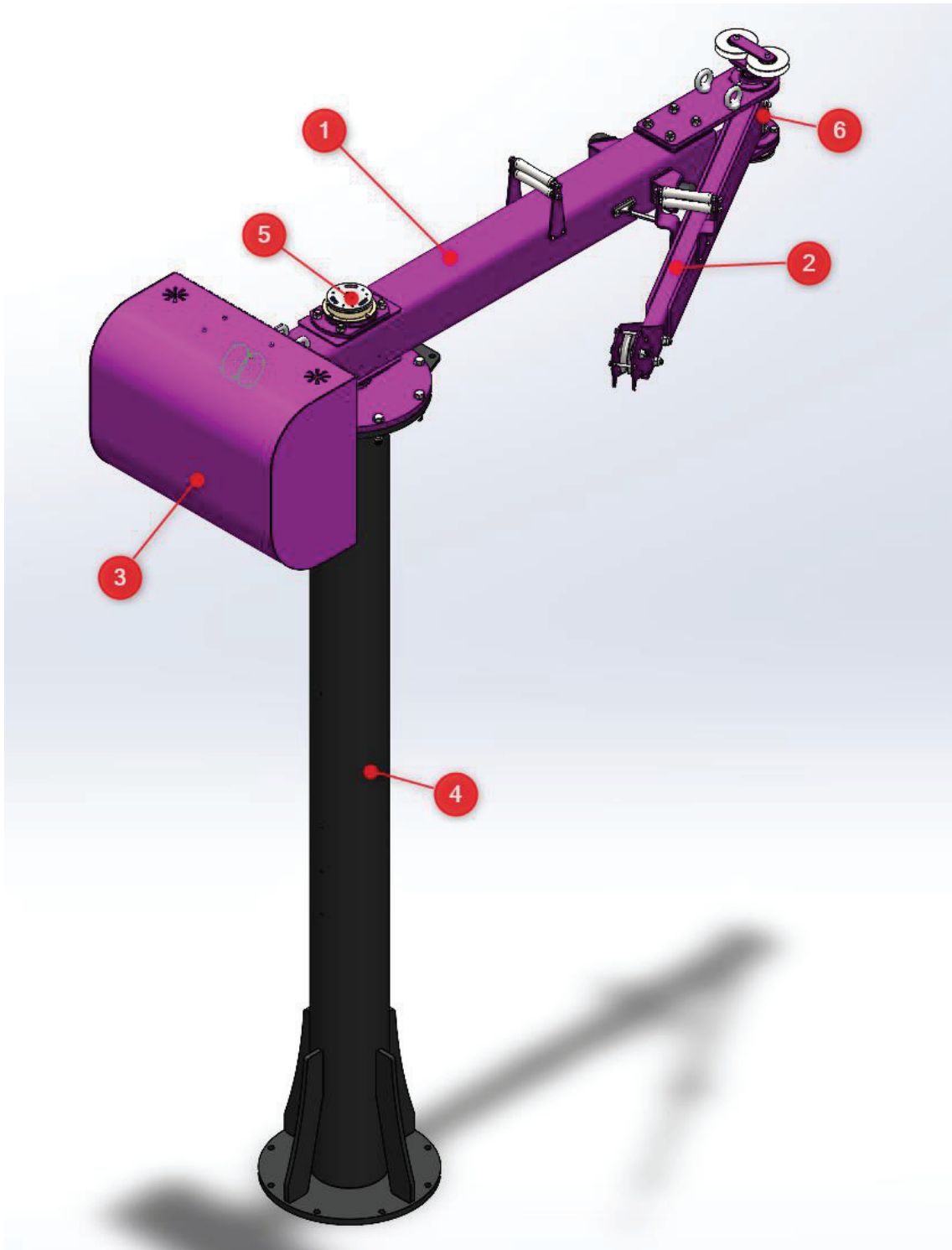


Figure 12: Design of the construction.

A manufactured picture of the construction is given in Figure 13.



Figure 13: Manufactured picture of the construction.

### 3.2. Design Requirements

The design requirements for the physical human-robot interface consist of mechanical strength, size, and mass, respectively. Also, the system must include a death man switch on the handle and an emergency stop button for safety reasons. The system

must have analog readings for the vertical speed input and must include a payload sensing component for the admittance control option.

Since the operator is near or under the load, all the load carrying elements including the handle system should have a minimum 10 factor of safety. Also, the materials that have been used for the load carrying elements must have a ductile property. The maximum load capacity of the system is 300 Kg so, the physical human-robot interface must have 10 or higher factor of safety under the 300 Kg load.

The size limits cover the maximum dimensions of the physical human-robot interface design. The total length of the system from wire rope to the hook, should not exceed 700 mm, total width and depth of the physical human-robot interface should not exceed 200 mm. These dimensional limits are requested from the company so that, the end product should look similar to already existing physical human-robot interfaces for lifting operations. In Figure 14, dimensional limits are shown on the industrial example of the physical human-robot interface. The length limit is shown as “L” and the width limit is shown as “W”.

Also, to use admittance type of control, the reactive force from the user interface to the operator should not exceed 30 Newton since the system will be controlled by the hand of the user.



Figure 14: Example of electrical physical human-robot interface  
(Source: Indeva Intelligent Devices for Handling, 2022)



The human-robot interface is located between the wire rope and the load so that it can measure the lifted load mass more accurately. This means that the electrical motor which is lifting the payload also must lift the physical human-robot interface. That is the reason why the physical human-robot interface should not exceed 10 Kg mass considering the idle power consumption. These design requirements are given below Tables as numerical and non-numerical to provide a better reading.

Table 1: Numerical design requirements

<b><u>Numerical Requirements</u></b>	
Minimum factor of safety	10
The payload capacity of the system (Kg)	300
Maximum Reactive Force (N)	30
Maximum length (mm)	700
Maximum width (mm)	200
Maximum depth (mm)	200
Maximum mass of the system (Kg)	10

Table 2: Non-numerical design requirements

<b><u>Non-numerical Requirements</u></b>
The system must include emergency stop
The system must include a hand presence sensor
Low stiffness user interface should be used
User can control the system by touching the payload

### 3.3. Mathematical Model

The mechanical stress which is acting on the human-robot interface can be classified as tensile stress since the wire rope automatically aligns the load vertically in the system. The load carrying element of the system is given in Figure 15:

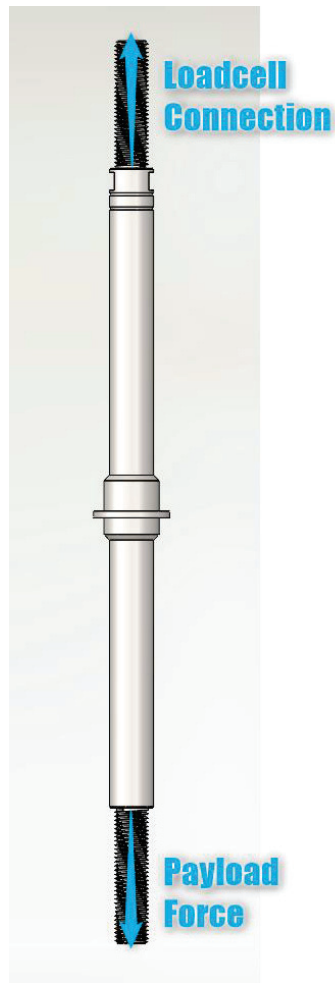


Figure 15: Load carrying element of the human-robot interface

Mechanical stress according to tensile stress is calculated following formulation:

$$\sigma = \frac{F}{A} \quad (1)$$

$$F = Mg \quad (2)$$

$$A = \pi r^2 \quad (3)$$

$\sigma$ : Total tensile stress

$F$ : Total force

$A$ : Total area

$M$ : Mass capacity of the system

$g$ : Gravity

$r$ : Effective radius

To calculate factor of safety following formulation is used:

$$n = \frac{\sigma_y}{\sigma} \quad (4)$$

*n: Factor of safety*

*$\sigma_y$ : Yields stress of the material*

By substituting Eq. 3 and Eq. 2 into Eq. 1 and then into Eq. 4, Eq. 5 is obtained.

$$n = \frac{\sigma_y \pi r^2}{Mg} \quad (5)$$

In equation 5, there are two parameters that we can manipulate:  $\sigma_y$  and  $r$ . However, material yield stress should be chosen first because of effective radius of the system can be adjusted more easily. Then, the radius of the load carrying bar can be adjusted according to linear bearing diameter and mechanical stress on the part.

In the sliding handle design, for the handle to come back to its original position, two compression springs are used. These springs work with opposite directions from each other and create a neutral point in the system. The proposed sliding handle design schematic is given in Figure 16.

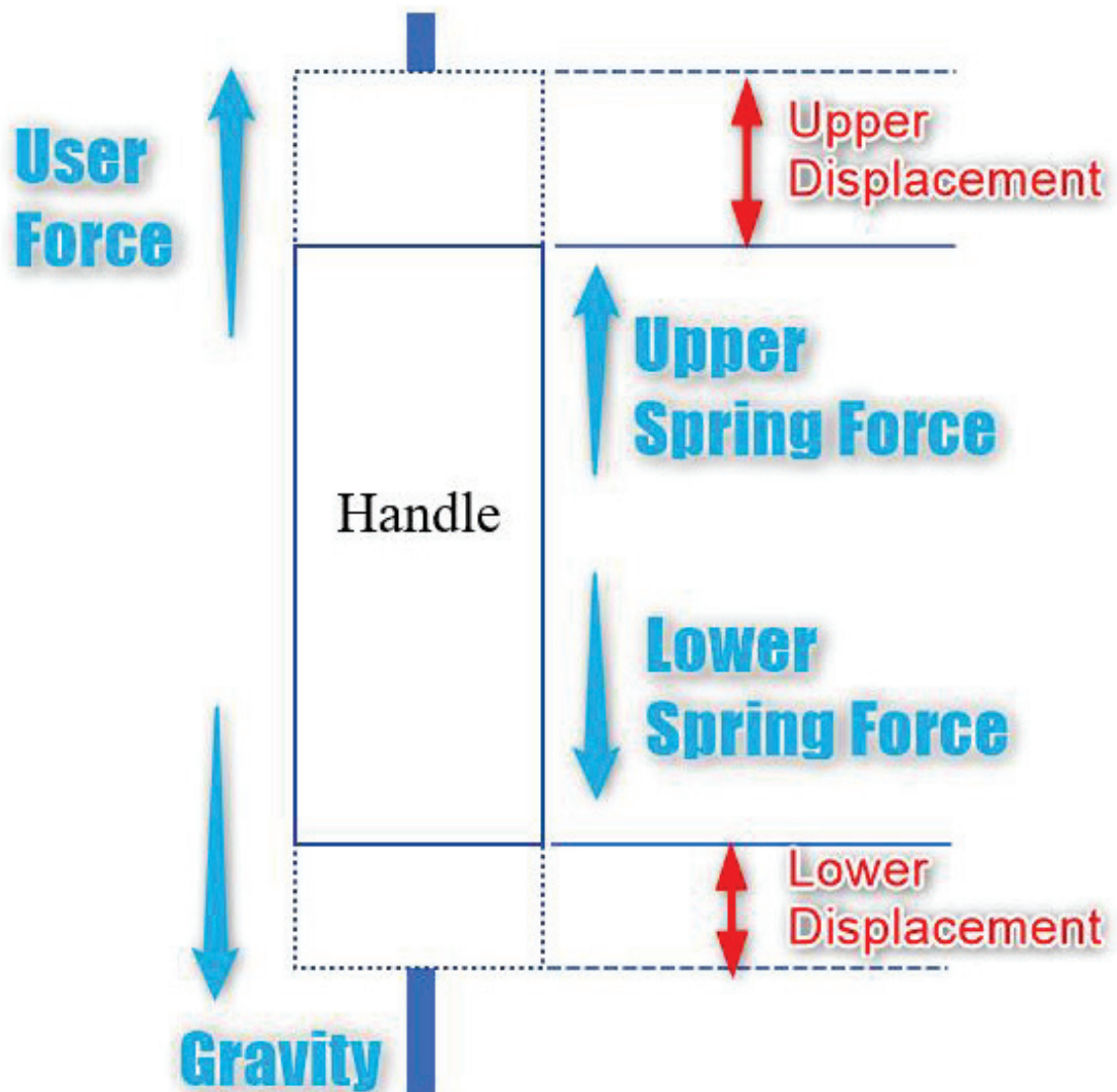


Figure 16: Sliding handle schematic

Spring formula as follow:

$$F_s = kx \quad (6)$$

$F_s$ : Spring force

$k$ : Spring constant

$x$ : Displacement

In the sliding handle system, mass of the handle and linear bearings should be included in the spring constant calculations. The forces that the operator feel will be the input and spring constants will be output in the following calculation.

$$F_o = F_1 - F_2 + mg \quad (7)$$

$F_o$ : Operator upward force

$F_1$ : Lower spring force

$F_2$ : Upper spring force

$m$ : mass of the sliding handle

By substituting Eq. 6 to Eq. 7, Eq 8. is obtained.

$$F_o = k_1(x_n + x_d) - k_2(x_n - x_d) + mg \quad (8)$$

$x_n$ : Neutral position displacement

$x_d$ : Displacement from neutral position

$k_1$ : Lower spring constant

$k_2$ : Upper spring constant

To calculate both spring constants we need two equations or two reference operator forces. As reference operator force, there are two scenarios. When no operator forces are acting on the handle, the handle should stay in its neutral position. When the deflection of the handle is maximum, the operator should feel the desired maximum force.

### 3.4. Design of the Load Carrying Element

Before designing a sliding handle, first load carrying elements should be selected and designed. The material choice would be the first step in designing a system since the yield strength and elasticity of the material will be critical. Aluminium and steel materials are the most used in industry for ductile property and relevant high strength. Aluminium metals have a higher mass-to-strength ratio over the steel metals but, in terms of volume,

steel metals have an advantage. Since our volume is more limited than the mass limit, DIN C35 steel is selected.

After the material selection, the effective minimum diameter can be calculated. By using equation 5, the load carrying element radius should have a 4.72 mm or higher value for, the desired factor of safety 10 with 420 MPa yield strength (“C35 / 1.0501 Equivalent, Properties” 2011) under the 300 Kg load. To assemble the load carrying bar to the load cell and the hook, metric threads are used. With this minimum effective radius value, the M12x1.75 metric thread is selected.

The final properties and results are listed below.

Table 3: Design properties of the load carrying bar.

Material	DIN C35
Yield Strength (MPa)	420
Material Standard	EN 10083-2
Effective Radius (mm)	4.93
Factor of Safety	10.9

### 3.5. Design of the Sliding Handle

To design a low stiffness admittance type of control interface, user sense and user input force are the most important factors to be considered in the design parameters. Another factor to be considered is to measurement method for the displacement of the handle. The system needs an analog value from the sensor that reads the displacement of the handle but, to read a displacement there are different sensor and measurement techniques to be considered.

### **3.5.1. Sensor Selection**

In the industry most of the sensors work with 24V and analog signal output ranges can be 0-10V or 0-20mA. As a result of that, the PLC controller that is used in the system expects analog values in this range. Another parameter will be the resolution of the sensor since the higher resolution would result in better control of the vertical speed.

Any optical-based sensor cannot be used in the system since it can be disturbed by the environmental effect. This problem eliminates optical cameras, laser, and infrared sensors to be used in the system. To eliminate this kind of disturbance, a mechanically connected sensor is needed.

To solve the problem mentioned above, a rotatory potentiometer is selected. With this type of sensor, the system has an infinite resolution about the displacement measurement, and it cannot be disrupted by environmental effects.

### **3.5.2. Prototype Design**

With the selection of the materials and sensors, designing the prototype is initiated. The prototype design is aimed to control the up-down movement of the system and test the springs system that is used in the sliding handle mechanism. The selection of the displacement sensor creates a problem in the design. The rotatory potentiometer can measure rotatory motion but the measurement which the system required is a linear motion.

To convert linear motion to rotatory motion, a slider crank mechanism is selected. Since this prototype will only be used as a conceptual design, it doesn't need all the design requirements and it aimed to demonstrate low stiffness admittance type of control system can control the vertical speed of the system. In Figure 17, a section view of the prototype design can be seen and in Table 4, component descriptions are given with their respective number.

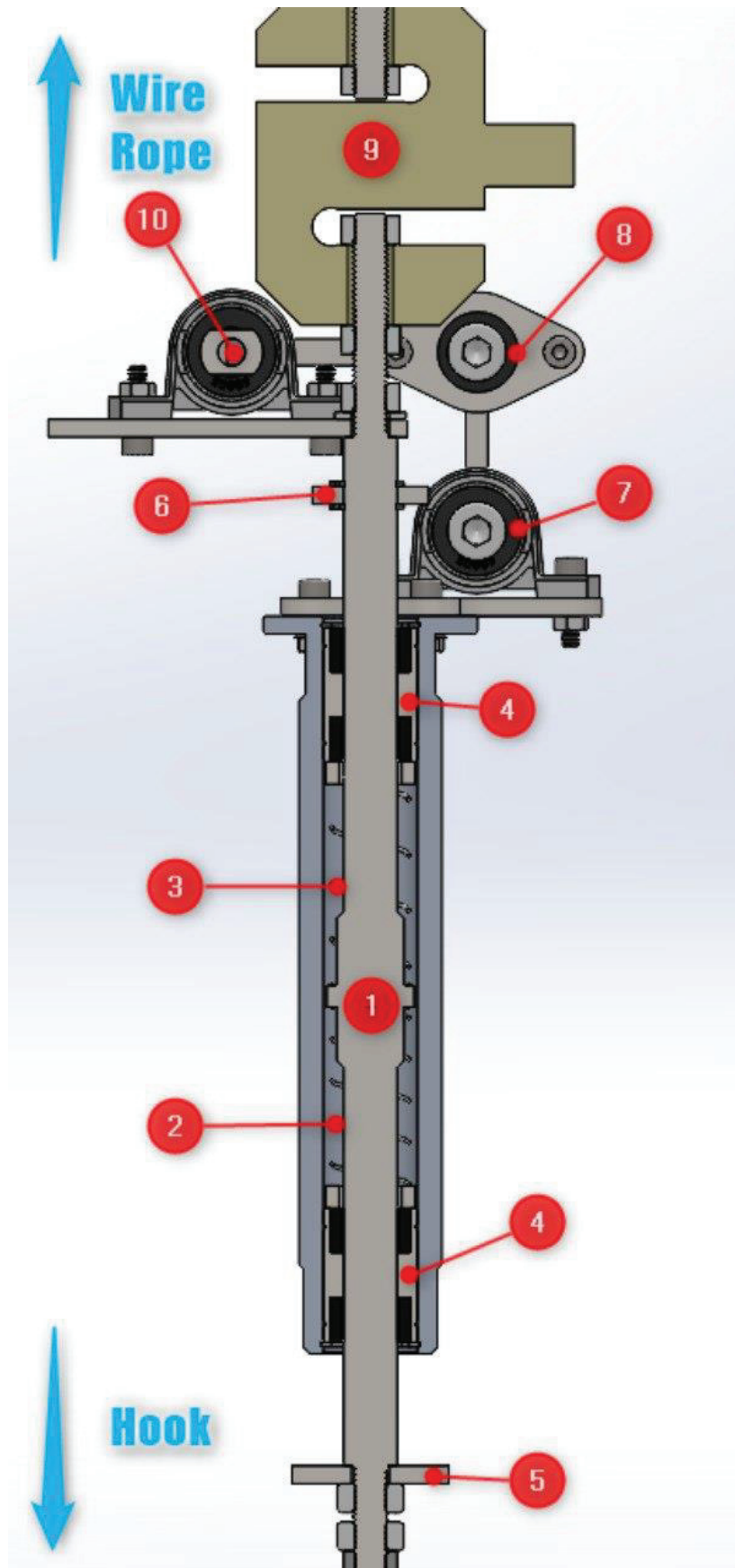


Figure 17: Section view of prototype design



Table 4: Description of the sliding handle mechanism prototype elements

<u>Number</u>	<u>Description</u>
1	Load Carrying Bar
2	Lower Spring
3	Upper Spring
4	Linear Bearings
5	Lower Stopper
6	Upper Stopper
7	KP 08 Bearing
8	KFL 08 Bearing
9	Load Cell
10	RCS 3100 Angle Sensor

The components used in the prototype design are listed below with their properties.

- Linear bearings are selected to reduce linear friction on the sliding handle.
- KP 08 and KFL 08 pillow block bearings are selected to eliminate bedding problems.
- RCS 3100 rotatory potentiometer is used.
- In the linkages, to manufacture easily sheet metals are used.

The handle displacement limit is selected as 25mm in one direction. This displacement value was requested from the company. With this displacement value, spring constants selection is done using Equation 8.

- Mass of the handle including linkages: 0.5 Kg
- Maximum reaction force of the system: 0.5 Kg
- Maximum deflection of the handle: 25mm
- Springs nominal length: 100mm
- Springs compression under neutral position: 55mm

Using above mentioned restriction following equations are used:

$$0 = k_1 55 - k_2 55 + 4.905 \quad (9)$$

$$4.905 = k_1 80 - k_2 20 + 4.905 \quad (10)$$

Solving Equations 9 and 10, the upper and lower spring constants are found as:

- Lower Spring constant:  $k_1 = 0.03 \text{ N/mm}$
- Upper Spring constant:  $k_2 = 0.119 \text{ N/mm}$

Assembled photos of the prototype sliding handle mechanism can be seen in Figure 18.

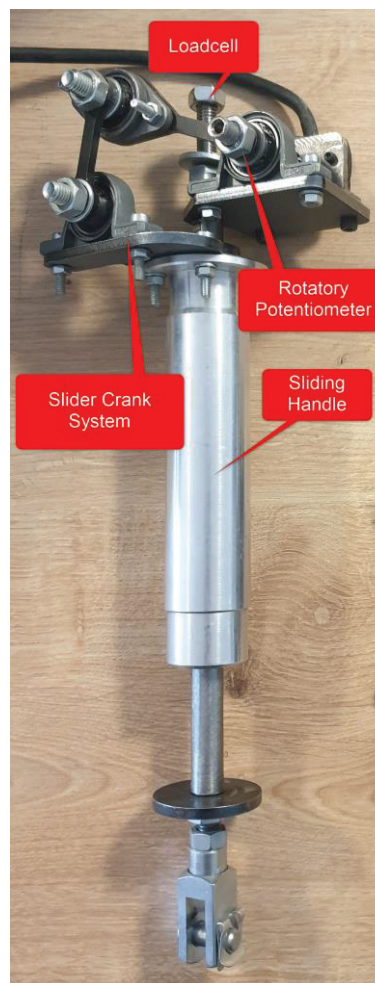


Figure 18: Picture of the assembled prototype sliding handle mechanism

## CHAPTER 4

### FINAL DESIGN AND TESTING OF THE PHYSICAL HUMAN-ROBOT INTERFACE

In this chapter, testing of the sliding handle mechanism and the final design of the system are covered. The prototype design is tested and according to test results, the final design of the user interface is improved. After that final test of the system is conducted.

#### 4.1. Testing of the Prototype Design

These test procedures are about the springs and their performance in the system. If one of the spring's performances is under or over, the handle neutral position will deviate from the desired position. The test rig of the system can be seen in Figure 19. In Figure 19, the prototype design of the physical human-robot interface is connected to the motor using wire rope and 20, 50 and 80 kg payloads are attached to the system. The motor which is used in the testing is an AC motor which is connected to the reduction gear and a drum. This assembly stimulates the power system in the lifting system. Since the power system is only used for vertical motion, in the test system there is no need for horizontal movement. The test system parts are listed below:

1. Power system: Includes 0.75 Kw AC motor which can lift to 100 Kg of payload.
2. Wire rope: 5 mm wire rope
3. User interface
4. Lifting magnet: To attach the metal payload to the hook.
5. Payload: 20, 50 and 80 kg of sheet metals.

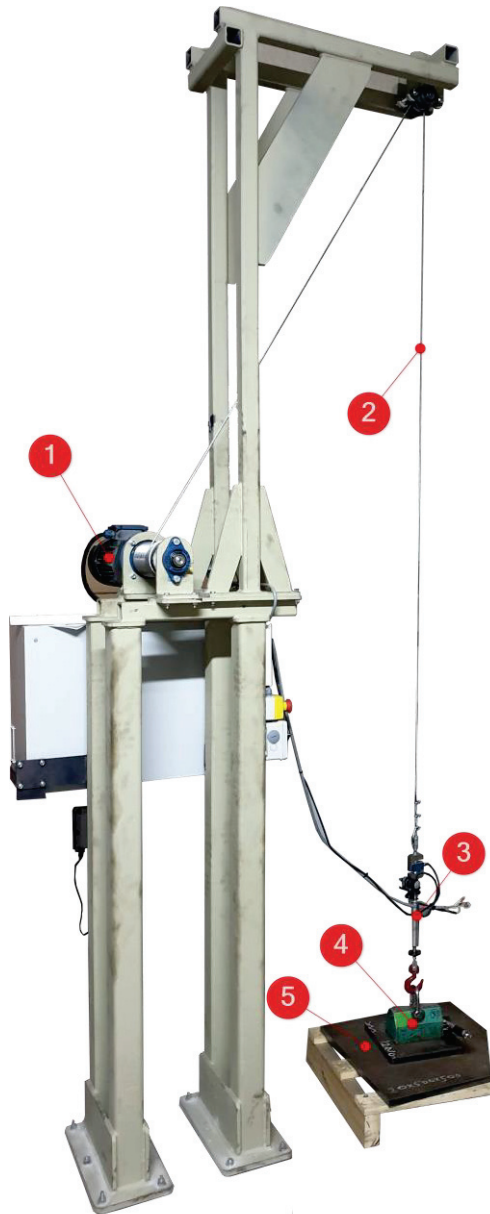


Figure 19: Test system of the prototype human-robot interface.

#### 4.1.1. Force Test of the Prototype

In this test, the reactive force of the low stiffness force measurement system is measured using a force sensor. The system is lifted into the air, and the reactive forces of the springs are measured at the max displacement points of the handle. The result of the measurement is given in Table 5.

Table 5: Force test results of the prototype design

Displacement of the Handle (mm)	Measured Force (Kg)	Expected Force (Kg)
+25	0,505	0,500
+25	0,500	
+25	0,505	
-25	-0,495	-0,500
-25	-0,500	
-25	-0,510	

#### 4.1.2. Displacement Test of the Prototype

In this test, handle performance is measured. This test aims to find out if the handle will return to its neutral position after the operator releases the handle. This test is performed at four different points and the displacements are measured using a calliper. The result of the displacement test is given in Table 6.

Table 6: Displacement test results of the prototype design

Release Point Displacement (mm)	Return Point Displacement (mm)	Expected
+25	+0,5	0
+25	+0,2	0
+25	+0,3	0
+15	+10,2	0
+15	+9,8	0
+15	+10,3	0
-15	-11,1	0
-15	-10,5	0
<b>(cont. on next page)</b>		

<b>Table 6 (cont.)</b>		
-15	-10,7	0
-25	-0,3	0
-25	0,0	0
-25	-0,1	0

### **4.1.3. Mass Measurement Test of the Prototype**

In this test, payload mass readings are measured under static conditions. Three different payloads are measured, and measurement processes are repeated three times. The system lifts the mass and after 1 second, measurement of the payload is carried out. The analog signal from the loadcell is converted into the mass of the payload by a mathematical formula. The results are listed below in Table 7.

Table 7: Mass test of the prototype design.

Payload Mass (Kg)	Measured Mass (Kg)
20	20.00
20	20.00
20	20.05
50	50.05
50	50.05
50	49.95
80	80.10
80	79.95
80	79.95

#### 4.1.4. Mass Measurement Test of the Wire Rope System

In this test, an industrial example model of a wire rope system that is measuring the mass of the payload with wire rope tension. For an industrial example, a crane system is tested, which can be seen in Figure 20. In Figure 20 isometric view of the crane system and the components that are needed for the test are given. Names of other parts in the picture are not given for confidentiality reasons.

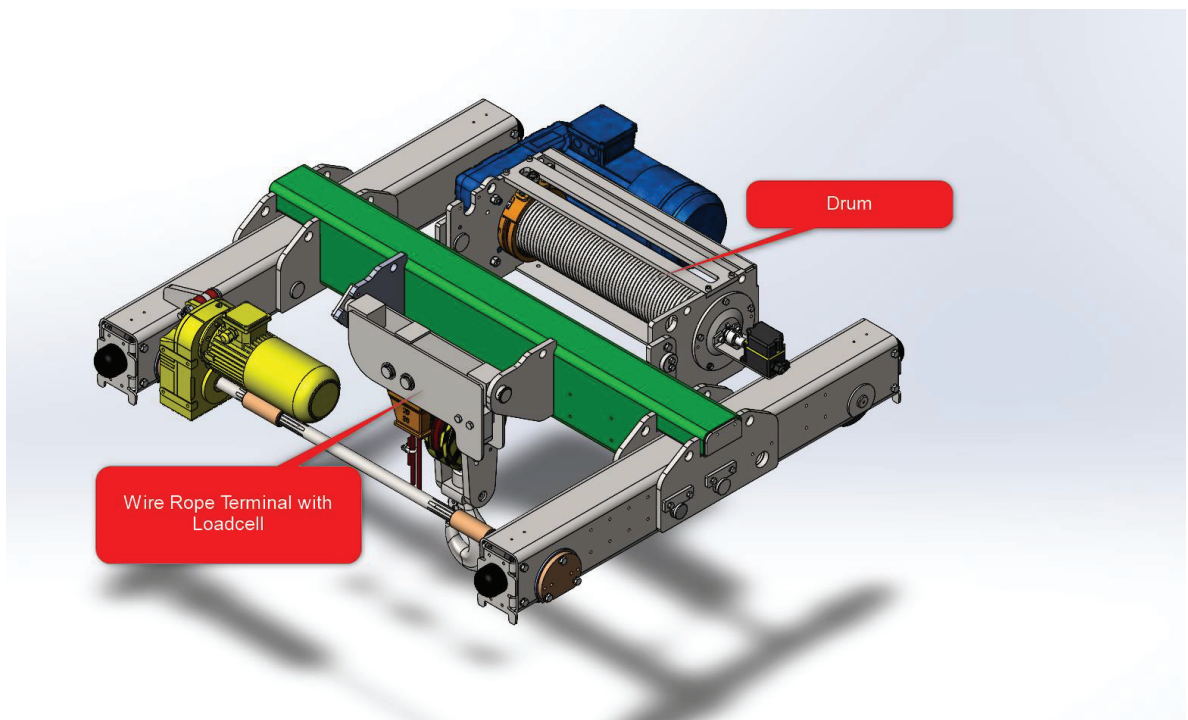


Figure 20: Example of a Crane System

The mass measurement method for the crane system is given in Figure 21. In this system, wire ropes follow the red arrow and its starts from the drum, after that the wire rope twist around the hook assembly and ends in the terminal. The load force is divided to two sides, the drum, and the terminal. The mass measurement is done on the wire rope terminal side.

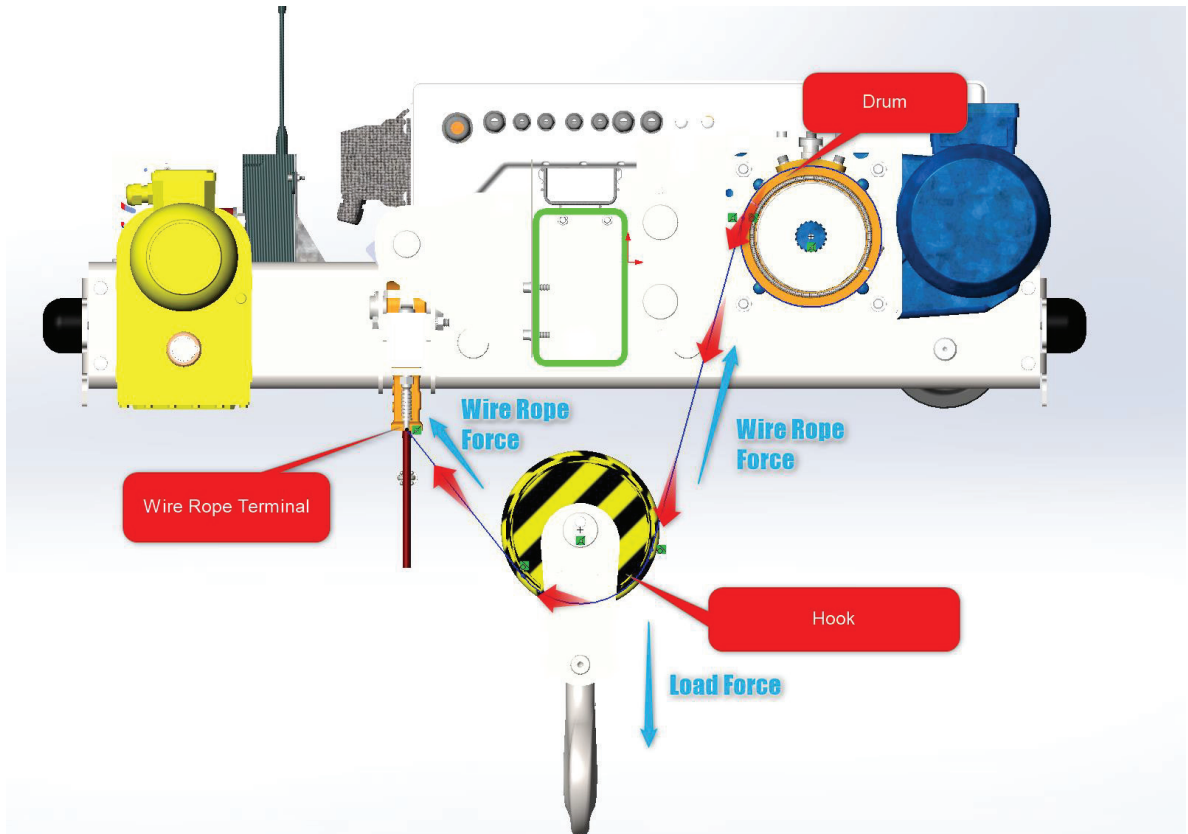


Figure 21: Wire Rope System

In wire rope terminal assembly, it includes a loadcell to measure the wire rope forces. The system uses a seesaw mechanism to transmit the wire rope forces to the loadcell. With this seesaw mechanism, if the loadcell breaks, the user does not lose control of the hook and the payload. The seesaw mechanism is given in Figure 22. The working principle of this measurement system is as follows: The payload mass creates a force in the wire rope, and this wire rope force is then transmitted to the wire rope terminal. In this terminal, because of the seesaw mechanism, the wire rope forces create a moment on the pivot point. This moment force is cancelled by the loadcell force on the system thus the mass measurement of the payload is completed.



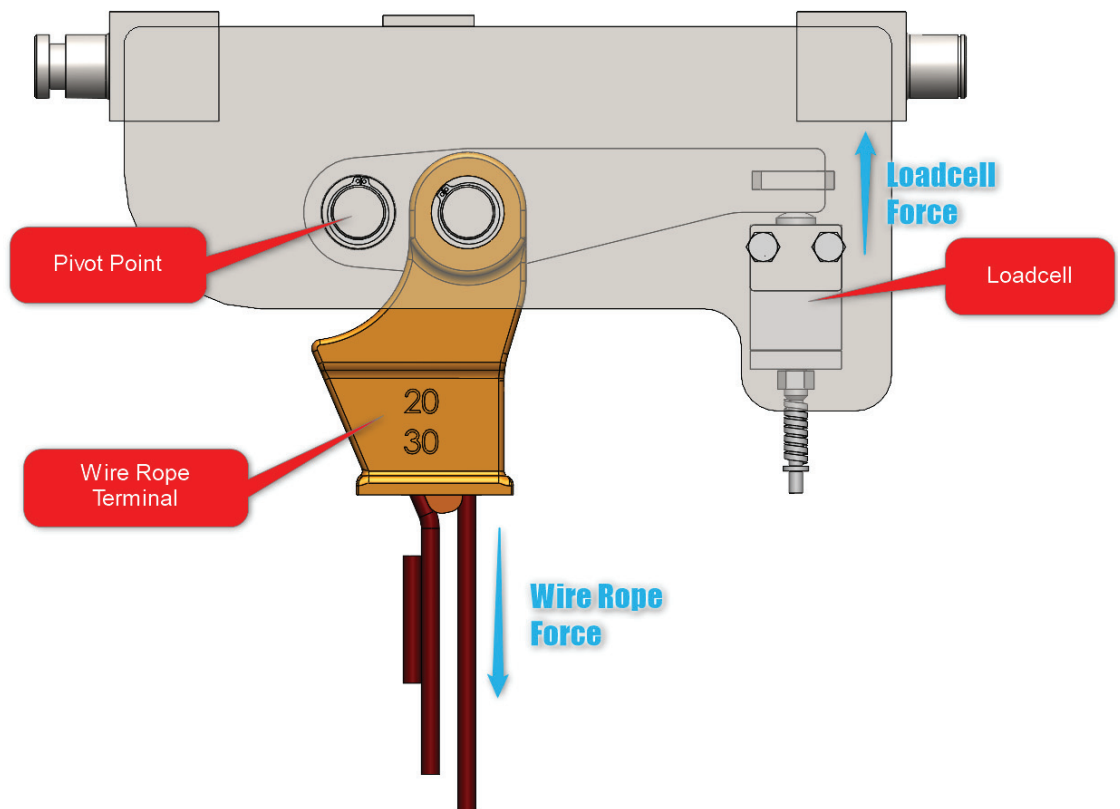


Figure 22: Seesaw Mechanism for Mass Measurement in Cranes

The same payloads are measured with this system and the results of the mass measurement of the test are given in Table 8.

Table 8: Mass test of the crane system.

Payload Mass (Kg)	Measured Mass (Kg)
20	22.1
20	18.7
20	21.5
50	51.3
50	50.9
<b>(cont. on next page)</b>	

<b>Table 8 (cont.)</b>	
50	47.8
80	82.3
80	81.2
80	79.6

#### **4.1.5. Discussion About Prototype Test Results**

Three different types of tests are performed on the prototype. These tests are aimed to measure the performance of the sliding handle mechanism and the loadcell. Force test results showed that the springs are performed as expected and mathematical models about spring constant calculations were correct. Mass test of the system results are showed that loadcell placement in the system can readout the payload mass without a problem and the measurements are better than the crane systems that measure the wire rope tension. Also, the electric motor power system showed that different masses can be lifted without making any adjustments from the user.

Displacement test results are showed that the system returns to its original position when it is released from maximum displacement but as the release point gets close to the neutral position, the handle is unable to return to its neutral position.

This displacement test result shows us that the friction on the system is high enough to counteract the spring forces. To solve this problem, there are two actions that can be taken: reducing the friction force and increasing the spring forces.

The main friction forces are coming from the bearings that are used in the slider crank mechanism. The pillow block bearing types have got increased friction since the radius of the core is higher. To solve this problem, bearings can be changed to deep groove ball bearings, but bedding problems could occur after the assembly or increasing the spring force could be done up to the maximum reactive force limit that is restricted by the design requirements.

## **4.2. Final Design of the User Interface**

In this section, improvements on the sliding handle mechanism and the final design of the physical human-robot interface are given. In the previous design, spring forces are not enough to overcome the friction in the system. This friction is mostly caused by the bearings in the system and to solve that problem, a new type of sliding handle mechanism is designed and manufactured.

### **4.2.1. Improvements**

To solve the friction problem, the number of bearings should be minimized. For this reason, using a slider crank design option is eliminated as well as using a rotary type of potentiometer. To measure linear displacement a linear sensor is chosen. This choice was not originally considered because almost all of the linear potentiometers cannot deliver 0-10V analog values using 24V DC voltage. To get 0-10V analog values, the linear potentiometer needs a 10V DC power supply, and this requires extra 2 cores in the cable. But this design choice will decrease the friction in the system and increase sliding handle performance.

### **4.2.2. Final Design**

With the test results of the prototype design, the final design of the physical human-robot interface is completed. In the final design, an emergency stop button and operator hand presence sensor is added to the system. Based on the test results of the prototype, spring forces were found to be low and had to be increased. In the new low stiffness force measurement system, reactive force is selected as 2 Kg at the maximum displacement. Also, since the upper spring must carry the handle mass, its spring constant must be much higher than the lower spring constant.

This phenomenon resulted in different coil diameters at the springs and creates another problem for the design. To accommodate this problem, the upper and bottom

spring's neutral lengths are selected differently. List of the final design features are listed below:

- Mass of the system: 6 Kg
- Length of the system: 540 mm
- Width of the system: 165 mm
- Depth of the system: 145 mm
- Mass of the handle: 0.55 Kg
- Maximum reaction force of the system: 2 Kg
- Maximum deflection of the handle: 25 mm
- Upper spring nominal length: 70 mm
- Lower spring nominal length: 75 mm
- Upper spring deflection at neutral position: 35 mm
- Lower spring deflection at neutral position: 35 mm

By using the above parameters and Equations 8, 11 and 12 were achieved.

$$0 = k_1 35 - k_2 35 + 5.3955 \quad (11)$$

$$19.62 = k_1 60 - k_2 10 + 5.3955 \quad (12)$$

Solving Equations 11 and 12, spring constants were found as:

- Lower Spring constant:  $k_1 = 0.317 \text{ N/mm}$
- Upper Spring constant:  $k_2 = 0.471 \text{ N/mm}$

With these improvements, all the design requirements are met, and the final design of the system can be seen in Figure 23 and, the section view of the design can be seen in Figure 24.

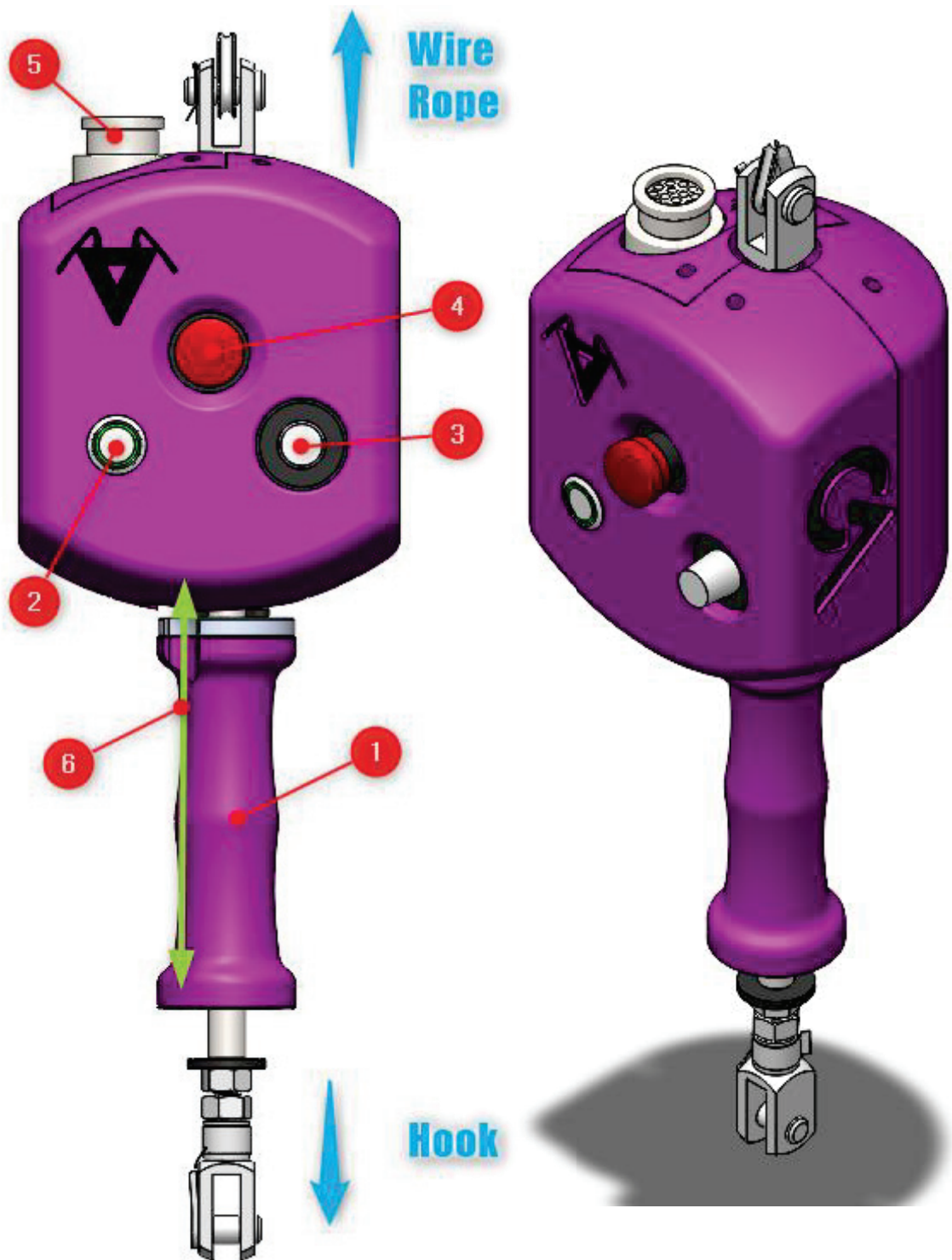


Figure 23: Front (left) and isometric (right) view of the human-robot interface.

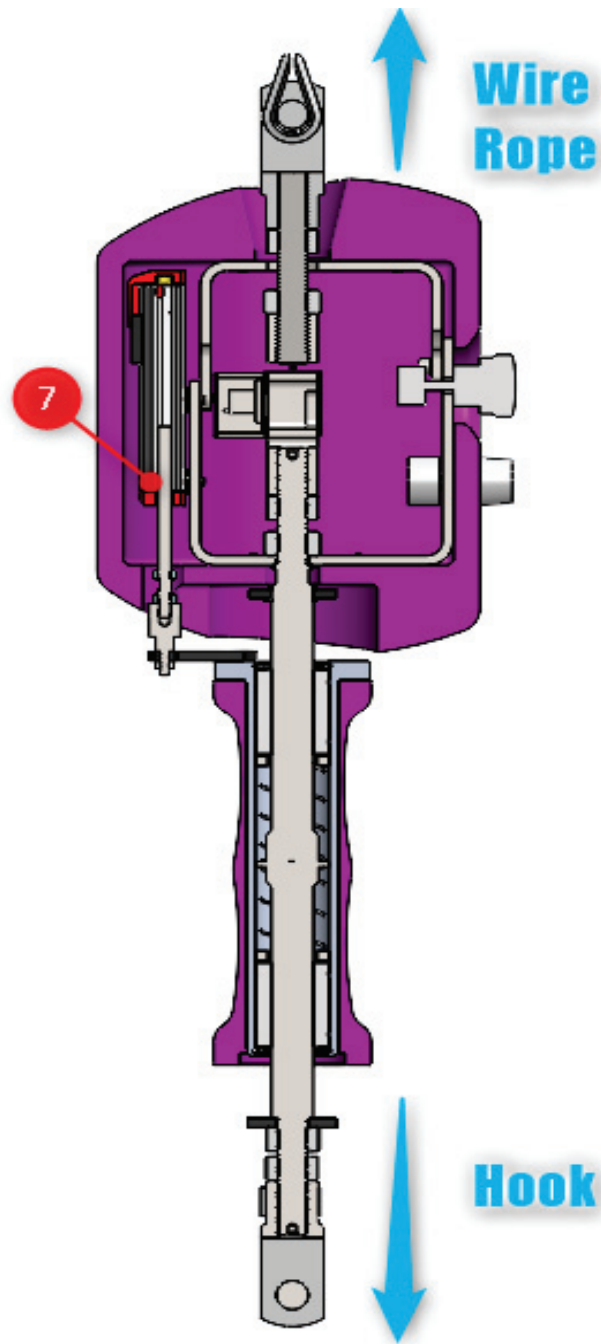


Figure 24: Section view of the final design.

Parts that were added to the new system are listed below:

1. Operator gripping interface
2. Admittance controller activation button
3. Speed adjuster of the system
4. Emergency stop button

5. Electrical plug
6. Human hand presence sensor
7. Linear potentiometer

After the design processes manufacturing of the physical human-robot interface is done and the final product pictures can be seen in Figure 25.



Figure 25: Final product picture of the physical human-robot interface

The integrated assembly of the human-robot interface with the construction can be seen in Figure 26:

1. User interface
2. Power System
3. Wire rope

4. First Arm
5. Second Arm
6. The mast

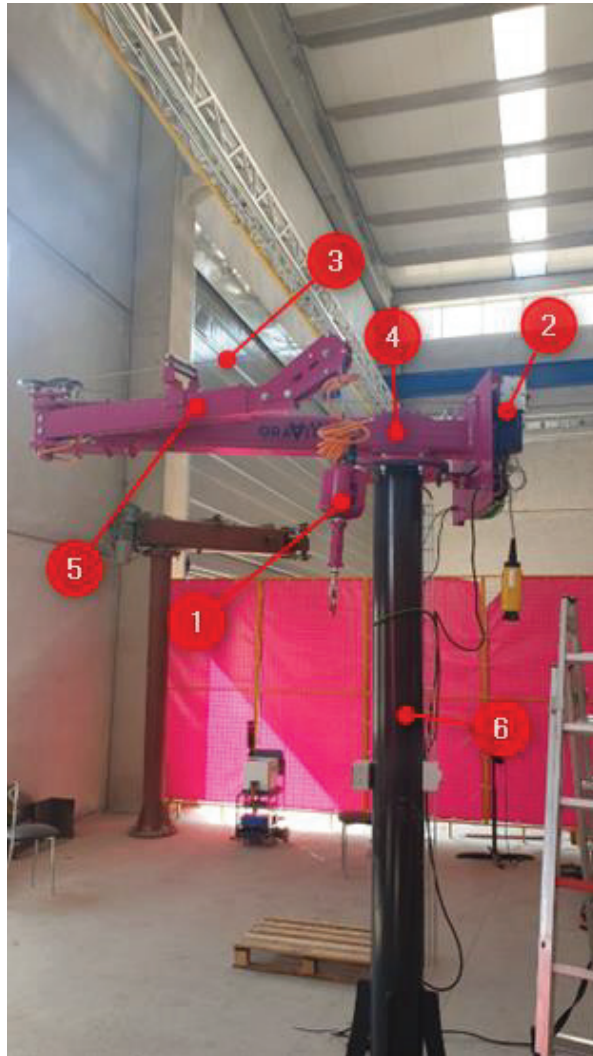


Figure 26: Assembled picture of the lifting system with human-robot interface

### 4.3. Test and Results of the Final Design

The test procedure of the final design is the same as the test procedure of the prototype design. The test rig and the test mass of the system are the same as the prototype design test which can be seen in Figure 19. The result of the mass, force and displacement measurement tests are shown in Tables 9, 10 and 11 respectively.



Table 9: Force test results of the final design of the physical human-robot interface

Displacement of the handle (mm)	Measured Force (Kg)	Expected Force (Kg)
+25	2,010	2
+25	2,005	
+25	2,005	
-25	-2,000	-2
-25	-2,005	
-25	-2,010	

Table 10: Displacement test results of the final design of the physical human-robot interface

Release Point Displacement (mm)	Return Point Displacement (mm)	Expected (mm)
+25	+0,1	0
+25	0,0	0
+25	-0,1	0
+15	+0,2	0
+15	+0,1	0
+15	+0,2	0
-15	-0,3	0
-15	-0,1	0
-15	-0,1	0
-25	0,0	0
-25	-0,1	0
-25	0,0	0

Table 11: Mass measurement test of the final design

Payload Mass (Kg)	Measured Mass (Kg)
20	20.05
20	19.95
20	20.00
50	49.90
50	50.05
50	50.00
80	80.05
80	80.10
80	79.90

#### 4.4. Surface Impact Test with Using Both Control Methods

In this test, the surface reaction forces of both high and low stiffness admittance control types are measured. To compare both systems an accelerometer is placed on the hook and measures the vertical g-forces acting on the user interface. For a payload, a 30 Kg steel part is used and connected to the hook by a magnet. The test procedure is as follows; The operator lifts the payload about 10 cm from the table and rests the system for 10 seconds. After the system settles down, the accelerometer recording is started, and the operator uses both control methods to place the payload back on the table. The test system can be seen in Figure 27.

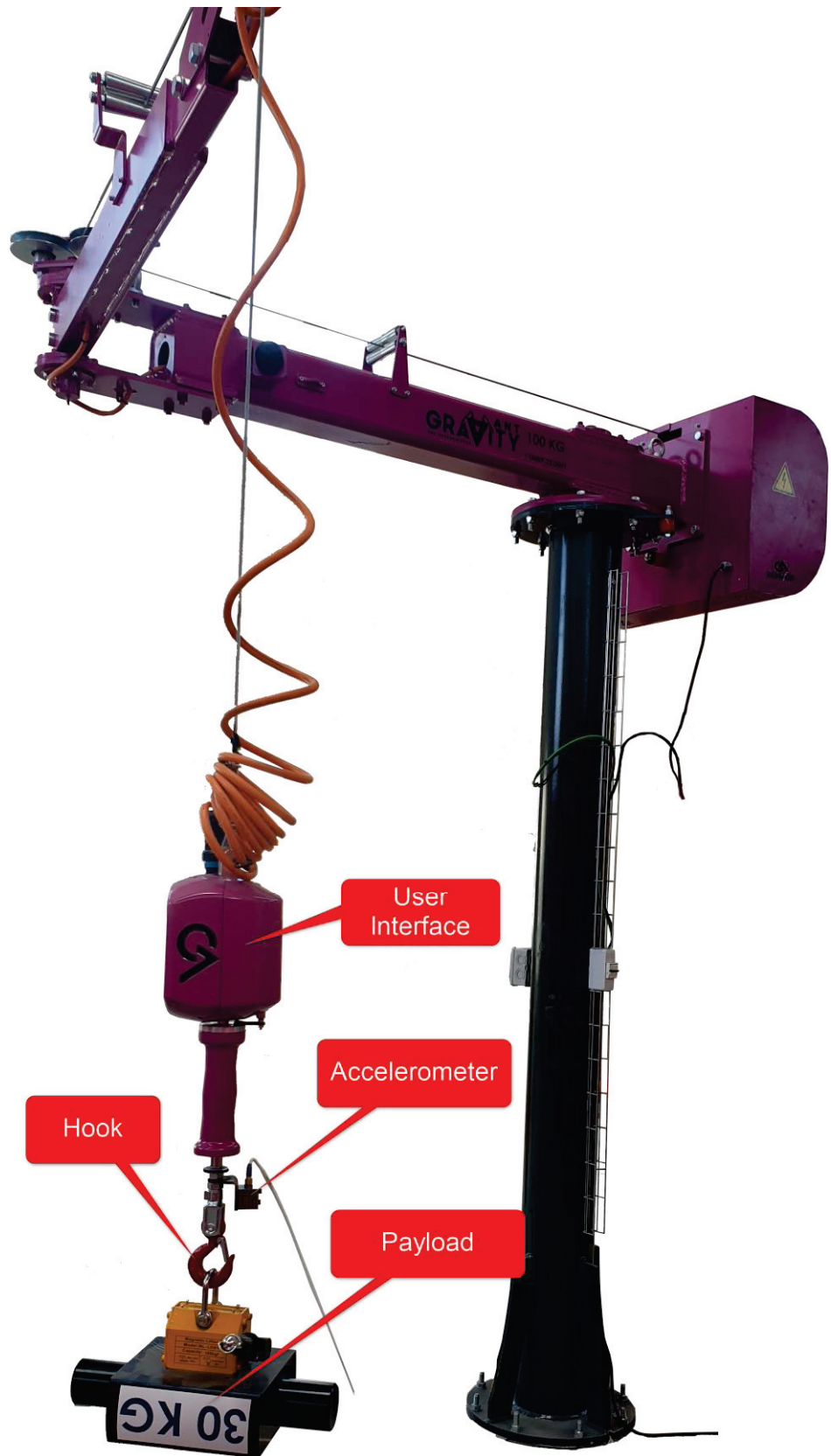


Figure 27: Surface Impact Test System

#### 4.4.1. High Stiffness Admittance Control Test

This method uses loadcell reading to calculate operator forces on the payload and according to the user payload, the vertical movement of the system is controlled. With this control method, 30 Kg of steel part is placed on the surface and the surface impact g-forces were measured. The test results can be seen in Figure 28. To see surface impact forces clearly, the time interval is shown only for the surface impact region.

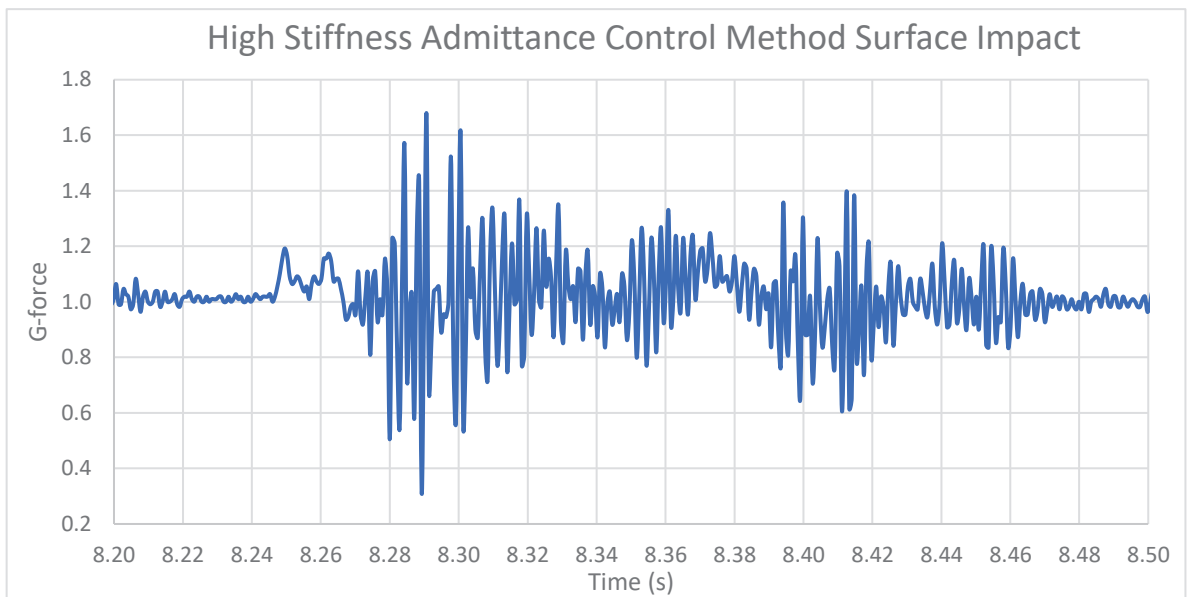


Figure 28: High Stiffness Admittance Control Method Surface Impact Test

In Figure 28, the first surface contact appears on time 8.25 seconds and the resulting g-force is about 1.2 g. After the initial contact, the payload still moving in the downward direction and about 0.05 seconds later the oscillations begin. The peak g-forces can reach up to 1.676 g-forces and the oscillations lasted about 0.22 seconds.

#### 4.4.2. Low Stiffness Admittance Control Test

This method uses handle displacement readings and according to the displacement values, the vertical movement of the system is controlled. With this control method, 30 Kg of steel part is placed on the surface and the surface impact g-forces were measured. The test results can be seen in Figure 29. To see surface impact forces clearly, the time interval is shown only for the surface impact region.

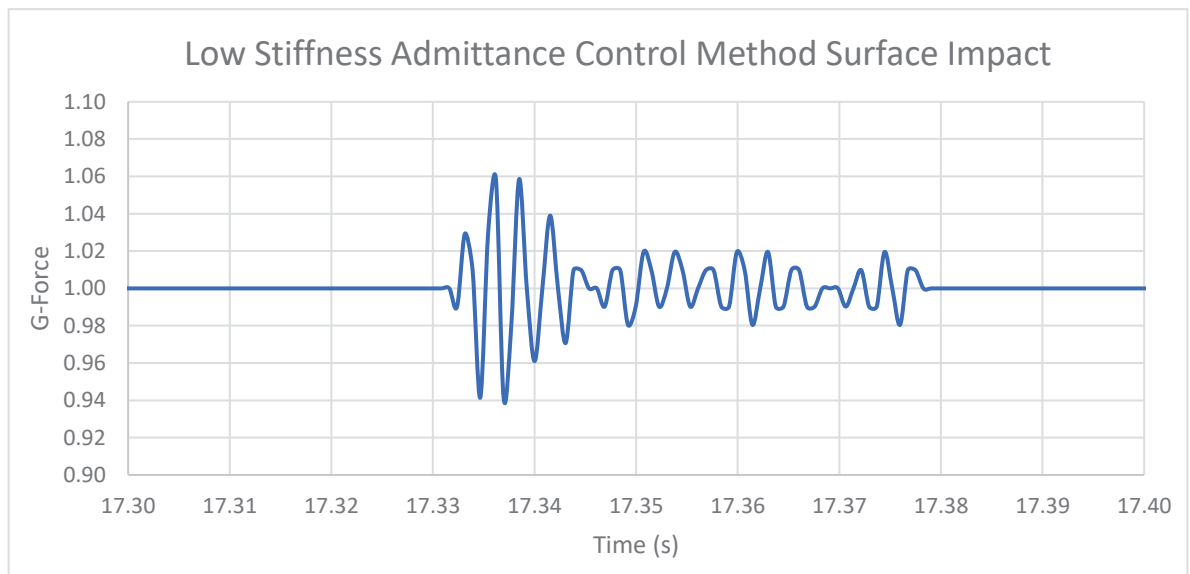


Figure 29: Low Stiffness Admittance Control Method Surface Impact Test

In Figure 29, the first contact appears on time 17.332 seconds and the resulting g-force is about 0.99 g. After the initial contact oscillations continue for 0.05 seconds and the peak g-force is 1.06 g-force.

#### 4.5. Discussion About Final Design Test Results

According to prototype test results, springs and loadcell performance are within the expected parameters but the friction on the system is prevented the sliding handle mechanism return to its original position. To solve this problem, a new type of sliding

handle mechanism is designed and manufactured. Also, spring forces are increased to overcome friction in the system.

In the force test results, increased spring forces do not affect the performance of the springs and measurements are similar to the prototype design. Since the loadcell position in the final design is not changed, the force measurements of the new design are not affected by the sliding handle design changes. The main improvement in the final design is to solve displacement errors in the sliding handle system. In the displacement test results of the final design, it is seen that displacement errors are highly reduced in the low displacement areas.

To compare both force reading methods, a surface impact test is conducted. This test aimed to show the surface impact forces which occur when the payload touches a surface. High stiffness admittance control method test is conducted to show the current control method surface impact forces. In the admittance test result, it is seen that the peak g-forces can go up to 1.67 g-force and the oscillations last about 0.22 seconds. On the other hand, low stiffness admittance control test results are much better and smoother than the high stiffness admittance test results. In the low stiffness test, the peak g-force goes up to 1.06 g and oscillations last about 0.05 seconds. With this result, the design of the physical human-robot interface is completed according to design criteria.

## CHAPTER 5

### CONCLUSION

In this study, the design of the physical human-robot interface was presented. In this design, low stiffness admittance type of control method was used other than the high stiffness admittance type of control method which is widely used in the industry. With this type of control, the proposed system aimed to reduce the surface impact of the payload and provide better control for the operator.

In the literature survey, the problem with the high stiffness admittance type of control was studied and developments in electrical manipulators and their advantages were given. The most important feature of the electrical manipulator is that it can lift any mass up to its mass limit without making any adjustments to the system. With this feature, electrical manipulators have started to take place in the industry. Even though the system takes place in the industry for 20 years, there are still improvements that can be made to the product that can improve operator control and payload safety.

Lifting different masses without making any adjustments is the main problem with pneumatically controlled lifting systems. In the designed physical human-robot interface the lifting operations are carried out with electrical motors which use their own control algorithms to adjust lifting forces. This way, the user does not need to make any adjustments to lift different payloads.

The main problem with the electrical manipulator is the surface impact forces that could generate unwanted behavior in the system. To solve this problem, a low stiffness admittance type of controller is introduced to the system with using a sliding handle design. According to the design requirements and mathematical models, a prototype was manufactured and tested. In the test results, friction on the system was too high that it affected sliding handle performance. To accommodate this problem, spring forces were increased, and a new type of sliding handle design was introduced into the system.

With this new design, low stiffness admittance type of control interface is achieved but the high stiffness of the admittance cannot be overlooked. In the system, the high stiffness admittance type of control can be activable if the operator is desired. The

high stiffness admittance type of control is achieved in this design with the placement of the load sensor. This sensor is carried out by the measurements of the payload mass and operator forces on the payload. With this method operator can control the payload with touching the payload rather than the using the control interface.

To see the different control methods surface impact forces, a surface impact test is carried out. In the test results, it is seen that the low stiffness admittance control method is reduced the surface impact force by a factor of 10 and the oscillations after the surface impact are reduced by a factor of 5. This test results with the mass measurement test results are showed that the main objectives of this thesis are accomplished.

Finally, the design of the physical human-robot interface is completed and found to be suitable to be used in lifting operations.

## **5.1. Future Works**

For future works, the physical human-robot interface will be connected to the power system and integrated tests could be done to verify its performance under dynamic conditions. These tests are about the control methods that are used in the motor controller which can affect the performance of both control types. Changing the motor controller gains to tune the surface reaction forces and dynamic reactions of the system can be done.



## REFERENCES

- Adams, Richard J., and Blake Hannaford. 1999. "Stable Haptic Interaction with Virtual Environments." *IEEE Transactions on Robotics and Automation* 15 (3): 465–74. <https://doi.org/10.1109/70.768179>.
- "C35 / 1.0501 Equivalent, Properties." 2011. 2011. [http://www.steelnumber.com/en/steel\\_composition\\_eu.php?name\\_id=150](http://www.steelnumber.com/en/steel_composition_eu.php?name_id=150).
- "Dalmecc Industrial Manipulators." 2022. 2022. <https://www.dalmecc.com/manipulators/partner-ps/>.
- "GURALP Crane and Machinery." 2017. 2017. <https://www.guralpvinc.com.tr/dokumanlar.php>.
- Hogan, Neville. 1989. "Controlling Impedance at the Man/Machine Interface." *Proceedings - IEEE International Conference on Robotics and Automation*, 1626–31. <https://doi.org/10.1109/ROBOT.1989.100210>.
- "Indeva Intelligent Devices for Handling." 2022. 2022. <https://www.directindustry.com/prod/scaglia-indeva/product-5527-2018289.html>.
- Kazerooni, Hamayoon. 1999. Human Power Amplifier for Lifting Load Including Apparatus For Preventing Slack In Lifting Cable. US 6386513, issued 1999.
- . 2003. Human Power Amplifier for Lifting Load With Slack Prevention Apparatus. US 6886812, issued 2003.
- Keemink, Arvid Q.L., Herman van der Kooij, and Arno H.A. Stienen. 2018. "Admittance Control for Physical Human–Robot Interaction:" *https://doi.org/10.1177/0278364918768950* 37 (11): 1421–44. <https://doi.org/10.1177/0278364918768950>.
- Olsen, Raymond. 1964. Balanced Assembly. US 3134340, issued 1964.
- OSHA. 2009. "No Title." 2009. <http://osha.europa.eu/OSHA>.
- Ott, Christian, Ranjan Mukherjee, and Yoshihiko Nakamura. 2015. "A Hybrid System Framework for Unified Impedance and Admittance Control." *Journal of Intelligent*

*and Robotic Systems: Theory and Applications* 78 (3–4): 359–75.

<https://doi.org/10.1007/S10846-014-0082-1>.

Stockmaster, James. 2008. Lift Actuator. US 7559533, issued 2008.

Zanardi, Aldo. 2005. Apparatus For Lifting and Moving Objects. EP 1666400, issued 2005.